TOTAL POSITIVITY IN MULTIVARIATE EXTREMES

FRANK RÖTTGER[1], SEBASTIAN ENGELKE[1], AND PIOTR ZWIERNIK[2]

ABSTRACT. Positive dependence is present in many real world data sets and has appealing stochastic properties that can be exploited in statistical modeling and in estimation. In particular, the notion of multivariate total positivity of order 2 (MTP_2) is a convex constraint and acts as an implicit regularizer in the Gaussian case. We study positive dependence in multivariate extremes and introduce EMTP_2, an extremal version of MTP_2. This notion turns out to appear prominently in extremes, and in fact, it is satisfied by many classical models. For a Hüsler–Reiss distribution, the analogue of a Gaussian distribution in extremes, we show that it is EMTP_2 if and only if its precision matrix is a Laplacian of a connected graph. We propose an estimator for the parameters of the Hüsler–Reiss distribution under EMTP_2 as the solution of a convex optimization problem with Laplacian constraint. We prove that this estimator is consistent and typically yields a sparse model with possibly nondecomposable extremal graphical structure. Applying our methods to a data set of Danube River flows, we illustrate this regularization and the superior performance compared to existing methods.

1. INTRODUCTION

Multivariate dependence modeling for complex data relies on parsimonious models to avoid overfitting, allows for interpretation and enables inference in high dimensions. One approach to regularize models is the framework of conditional independence and sparsity (e.g., Lauritzen (1996); Wainwright and Jordan (2008)). While the sparsity assumption is often justified, fitting typically requires the choice of tuning parameters, and it may lead to suboptimal models. An alternative to this approach is the notion of positive dependence, which can also be seen as an implicit regularizer through a distributional constraint. Positive dependence has been extensively studied with connections to probability theory and statistical physics (Fortuin et al. (1971); Newman (1983, 1984)). In applications positive dependence arises naturally when the variables in the system are driven by common factors. Such situations occur, for example, in multivariate financial data, where the common factor can represent the intrinsic market component (Agrawal et al. (2020)). Another appearance is in evolutionary processes, where the observed variables evolve from a common ancestor (Steel (2016); Zwiernik (2018)).

Various mathematical definitions of positive dependence exist, including positive association (Esary et al. (1967)) and multivariate total positivity of order 2 (MTP_2) (Karlin and Rinott (1980); Fallat et al. (2017)). In particular, the latter notion is attracting a surging interest. The reason is that, for Gaussian models, it has the intuitive characterization that all correlations and partial correlations are nonnegative and that its analytical constraints on the distribution can be implemented elegantly in the estimation of statistical models (Slawski and Hein (2015); Lauritzen et al. (2019)). In addition, MTP_2 models outperform state-of-the-art methods in finance (Wang et al. (2020); Rossell and Zwiernik

(2021)), psychometrics (Lauritzen et al., 2019, 2021), machine learning (Ying et al. (2021); Egilmez et al. (2017)), medical statistics and phylogenetics Fallat et al. (2017). There is also a fundamental link between the assumption of sparsity and the MTP_2 constraint (Lauritzen et al. (2019)).

When interest is in extreme events, then intuitively one may expect even stronger positive dependence, as it can be conceived that multivariate extreme events arise from a common latent factor. For instance, during a financial crisis a shock may affect many stock prices simultaneously. Similarly, flooding at different locations is often caused by the same large-scale precipitation field.

Multivariate extreme value theory provides asymptotically motivated models for extremal dependence. Traditionally, the focus was on the analysis of max-stable distributions, which indeed can be shown to be always positively associated (Marshall and Olkin (1983)). Max-stable models arise as the componentwise maxima of independent copies of a random vector in its domain of attraction (de Haan and Resnick (1977)). This means that the latter can have any dependence structure, but the most extreme observations in each component eventually become positively associated. While this illustrates how positive dependence naturally emerges in multivariate extremes, max-stable distributions may be too rigid for modeling higher dimensional data. One reason is that their densities cannot factorize in a nontrivial way on graphs (Papastathopoulos and Strokorb (2016)).

The interest has, therefore, shifted to multivariate Pareto distributions, a different type of models in multivariate extremes, which are the only possible limits for multivariate threshold exceedances (Rootzén and Tajvidi (2006)). For this distribution class, extremal graphical models can be defined (Engelke and Hitz (2020)) that allow for sparse statistical models. In this paper we propose a new notion of positive dependence for multivariate Pareto distributions that we call extremal MTP_2 (EMTP_2).

As intuition from practice and the max-stable case suggest, EMTP_2 arises naturally in existing extreme value models. Indeed, we show in Section 3 that many classical models, such as the extremal logistic (Tawn (1990)) and extremal Dirichlet distributions (Coles and Tawn (1991)), are EMTP_2 across the whole range of their parameter values and in any dimension. Within multivariate Pareto distributions, the class of Hüsler–Reiss models (Hüsler and Reiss (1989)), parameterized by a variogram matrix Γ, can be seen as the counterpart of Gaussian models in multivariate extremes. An alternative parameterization is given in terms of the Hüsler–Reiss precision matrix Θ (Hentschel et al. (2022)). Inside this class we show that a model is EMTP_2 if its precision matrix is a Laplacian matrix of a connected graph with positive edge weights, that is, $\Theta_{ij} \leq 0$ for all $i \neq j$. This implies that any bivariate Hüsler–Reiss distribution is EMTP_2.

In Section 4 we formalize the connection between EMTP_2 distributions and graphical models for extremes. The case of Hüsler–Reiss distributions closely parallels Gaussian graphical models (Lauritzen et al. (2019)) but often allows for stronger results. For instance, all Hüsler–Reiss tree models are EMTP_2, and this even continues to hold for any latent tree structure. Finally, we study the axiomatization of extremal conditional independence in the spirit of Fallat et al. (2017) and Lauritzen and Sadeghi (2018) and show that EMTP_2 graphical models satisfy an extremal notion of faithfulness.

The methodological part of our paper focuses on the Hüsler–Reiss distribution. In Section 5 we propose an estimator of the Hüsler–Reiss precision matrix Θ that takes the empirical version of the variogram $\overline{\Gamma}$ as input and optimizes the convex problem

$$\text{(1)} \qquad \log \text{Det}\, \Theta + \frac{1}{2}\,\text{tr}(\overline{\Gamma}\Theta)$$

over all positive semidefinite precision matrices and under the EMTP_2 constraint that Θ is a Laplacian matrix of a connected graph with positive edge weights. Here Det denotes the pseudo-determinant since Θ has one zero eigenvalue. We prove the consistency of this estimator, and based on the

dual formulation, in Section 6 we design a block coordinate-descent algorithm that efficiently solves the constrained optimization problem. The EMTP_2 constraint acts as an implicit regularizer and the estimator can also be applied in high-dimensional settings. Moreover, since the solution satisfies KKT conditions for optimality, the estimator $\widehat{\Theta}$ under EMTP_2 typically contains zeros, which implies that the corresponding Hüsler–Reiss model is an extremal graphical model. We formalize this observation and show that the estimated EMTP_2 graph asymptotically is a super-graph of the true underlying graph. This allows for interpretation, in particular, when the estimated graph is sparse, as in our application to river networks in Section 7. We note that our estimator is the first method for extremal graphical models that goes beyond trees or block graphs (Engelke and Volgushev (2022)).

An important part of our theoretical contribution is the study of strong MTP_2, also known as LLC in the literature (Murota (2009); Robeva et al. (2021)). In order to characterize EMTP_2, we establish new additive relations of positive dependence, which are of independent interest. For a random variable X_0 that is independent of a random vector $\mathbf{X}$, we link the probabilistic dependence properties of

$$\mathbf{Z} = (X_0, \mathbf{X} + X_0 \mathbf{1}) \tag{2}$$

with those of $\mathbf{X}$, where $\mathbf{1}$ denotes the vector of ones. We will show that $\mathbf{Z}$ is MTP_2 if and only if $\mathbf{X}$ is strongly MTP_2. Models of the above form have been proposed under the name of random location mixtures (e.g., Hashorva (2012)). As we show later in the paper, this formulation also links to factor models (Lawley and Maxwell (1962); Krijnen (2004)). In the context of multivariate extreme value theory, these constructions produce versatile tail dependence structures. In the case of multivariate Pareto distributions, the so-called extremal functions are of the above form with a standard exponential variable X_0 and a lighter tailed random vector $\mathbf{X}$. Many models that bridge between asymptotic dependence and independence have a representation as in (2); see Engelke et al. (2019) for a review. In this paper we focus on asymptotic dependence and EMTP_2, but in Section 8 we discuss further implications of our theoretical results to asymptotically independent extreme value models.

To assess the statistical performance of our EMTP_2 estimator, in Section 7 we apply it to a data set of river discharges and compare it to methods from spatial statistics (Asadi et al. (2015)) and graphical modeling (Engelke and Hitz (2020)).

2. Background

Our paper is at the intersection of positive dependence modeling and multivariate extreme value theory. In this section we introduce the basic types of positive dependence constraints, and we review existing results on multivariate Pareto distributions and their connections to extremal graphical models.

2.1. **Notions of positive dependence.** We begin by recalling two notions of positive dependence. The first one is multivariate total positivity of order 2 (MTP_2) treated in detail in Karlin and Rinott (1980). The second is a stronger notion, which we call strong MTP_2 and whose study is motivated by the extremal MTP_2 property.

Let $\mathbf{x} \vee \mathbf{y}$ and $\mathbf{x} \wedge \mathbf{y}$ denote the componentwise maximum and minimum of $\mathbf{x}, \mathbf{y} \in \mathbb{R}^d$, respectively. A function $f : \mathbb{R}^d \to \mathbb{R}$ is *multivariate totally positive of order 2* (MTP_2) if

$$f(\mathbf{x} \vee \mathbf{y})f(\mathbf{x} \wedge \mathbf{y}) \geq f(\mathbf{x})f(\mathbf{y}) \quad \text{for all } \mathbf{x}, \mathbf{y} \in \mathbb{R}^d. \tag{3}$$

We say that f is strongly MTP_2 if

$$f\big(\mathbf{x} \vee (\mathbf{y} - \alpha \mathbf{1})\big)f\big((\mathbf{x} + \alpha \mathbf{1}) \wedge \mathbf{y}\big) \geq f(\mathbf{x})f(\mathbf{y}) \quad \text{for all } \mathbf{x}, \mathbf{y} \in \mathbb{R}^d, \alpha \geq 0, \tag{4}$$

where $\mathbf{1}$ denotes the vector of ones. A multivariate random vector $\mathbf{X}$ with density $f_{\mathbf{X}}$ is MTP$_2$ or strongly MTP$_2$ if the corresponding property holds for $f_{\mathbf{X}}$.

The concept of strong MTP$_2$ distributions is relatively new and not well studied. In the statistical context, Robeva et al. (2021) used (4) under the name of log-$L^{\#}$-concave (LLC) in reference to work on discrete optimization (e.g., Murota (2009)), where f is, in addition, assumed to be log-concave. For a list of further references for the appearance of strong MTP$_2$ in applications, see Robeva et al. (2021, pp. 3–4). The following important example discusses both notions of positive dependence for Gaussian distributions.

Example 1. If $\mathbf{X}$ is Gaussian with mean vector μ and invertible covariance matrix Σ, then $\mathbf{X}$ is MTP$_2$ if and only if the inverse covariance matrix K is an *M-matrix*, that is, a positive definite matrix such that $K_{ij} \leq 0$ for all $i \neq j$ (e.g., Lauritzen et al. (2019)). Moreover, $\mathbf{X}$ is strongly MTP$_2$ if, in addition, K is a diagonally dominant matrix, that is, all row sums are nonnegative ($K\mathbf{1} \geq \mathbf{0}$) (Robeva et al. (2021)).

Importantly, the MTP$_2$ property is closed under taking margins, under conditioning and under coordinatewise increasing transformations; see Corollary 3.3 and Proposition 3.4 in Fallat et al. (2017). Moreover, univariate distributions are always MTP$_2$.

The situation is more complicated for strongly MTP$_2$ distributions. In this paper we develop several new results for strong MTP$_2$ distributions that are central to the analysis of extremal MTP$_2$. First, we derive an alternative characterization of strong MTP$_2$ in Lemma B.1, which we employ in the proof of Theorem 3.1. This additionally implies that strong MTP$_2$ is also closed under taking margins (Proposition B.2). Furthermore, we show that univariate distributions are strongly MTP$_2$ if and only if the underlying density function is log-concave. This also shows that strong MTP$_2$ cannot be closed under arbitrary increasing transformations. Since these results are fairly technical, we postpone proofs and auxiliary results to Appendix B.

2.2. **Extremal dependence and multivariate Pareto distributions.** Multivariate extreme value theory studies the tail properties of a random vector $\mathbf{X} = (X_1, \ldots, X_d)$. The dependence between the largest values of each component, also called extremal dependence, quantifies to what degree rare events happen simultaneously in several variables. The full extremal dependence structure can be complex, and summary statistics are employed to condense this information into easily interpretable numbers. A popular bivariate summary statistic is the extremal correlation, defined for $i, j \in [d] := \{1, \ldots, d\}$ as

$$(5) \qquad \chi_{ij} := \lim_{q \to 0} \mathbb{P}\big\{F_i(X_i) > 1 - q | F_j(X_j) > 1 - q\big\} \in [0, 1],$$

whenever the limit exists and where F_j is the distribution function of X_j (e.g., Coles et al. (1999)). We speak of asymptotic dependence and independence if $\chi_{ij} > 0$ and $\chi_{ij} = 0$, respectively. The theoretical analysis for asymptotic independence is more nuanced, and a whole line of research exists (e.g., Heffernan and Tawn (2004); Wadsworth and Tawn (2012)); we discuss this further in Section 8. Extremal correlations can also be extended to higher dimension (Schlather and Tawn (2003)).

Since the univariate theory is well studied (e.g., Embrechts et al. (1997); de Haan and Ferreira (2006)), it is common to normalize the margins to concentrate on the extremal dependence. Throughout this paper we assume that each component of $\mathbf{X}$ has been normalized to have standard exponential distribution with distribution function $1 - \exp(-x)$, $x \geq 0$; we discuss this normalization in the preprocessing steps of the application in Section 7.1.

In this paper we focus on the case of asymptotic dependence. To describe the extremal dependence structure in this setting, the assumption of multivariate regular variation is widely used (Resnick (2008)). More precisely, we assume that the distribution of the exceedances of $\mathbf{X}$ over a high threshold

converges to a so-called multivariate (generalized) Pareto distribution $\mathbf{Y}$ (Rootzén and Tajvidi (2006)), that is,

$$\mathbb{P}(\mathbf{Y} \leq \mathbf{z}) = \lim_{u \to \infty} \mathbb{P}\big(\mathbf{X} - u\mathbf{1} \leq \mathbf{z}|\|\mathbf{X}\|_\infty > u\big), \quad \mathbf{z} \in \mathcal{L}. \tag{6}$$

The distribution of $\mathbf{Y}$ is supported on the space $\mathcal{L} = \{\mathbf{x} \in \mathbb{R}^d : \|\mathbf{x}\|_\infty > 0\}$, and it satisfies the homogeneity $\mathbb{P}(\mathbf{Y} \in t + A) = t^{-1}\mathbb{P}(\mathbf{Y} \in A)$ for any $t > 0$ and Borel set $A \subset \mathcal{L}$. We say that the vector $\mathbf{X}$ is in the domain of attraction of the multivariate Pareto distribution $\mathbf{Y}$. Note that assumption (6) is equivalent to multivariate regular variation of the random vector $\exp(\mathbf{X})$ (Resnick (2008), Proposition 5.15); see Remark 2.1 and Appendix C.1 for details.

Replacing the vector $\mathbf{X}$ in (6) by the Ith margin $\mathbf{X}_I = (X_i : i \in I)$, $I \subset [d]$, we denote the corresponding limit by $\mathbf{Y}_I$, which is a multivariate Pareto distribution on the space $\mathcal{L}_I = \{\mathbf{x} \in \mathbb{R}^{|I|} : \|\mathbf{x}\|_\infty > 0\}$. This is a slight abuse of notation since the so-defined random vector is not equal to the Ith margin $(Y_i : i \in I)$ of $\mathbf{Y}$ defined on $\mathbb{R}^{|I|}$. The difference between the two is only the support and restricting $(Y_i : i \in I)$ to $\mathcal{L}_I$ results in $\mathbf{Y}_I$.

Multivariate Pareto distributions $\mathbf{Y}$ are defined on the nonproduct space $\mathcal{L}$. In order to define stochastic properties for $\mathbf{Y}$, it is convenient to work with the conditional random vectors

$$\mathbf{Y}^k := \mathbf{Y}|\{Y_k > 0\},$$

where $k \in [d]$. If $\mathbf{Y}$ admits a Lebesgue density $f_{\mathbf{Y}}$, then $\mathbf{Y}^k$ has a density proportional to $f_{\mathbf{Y}}$ supported on the product space $\mathcal{L}^k = \{\mathbf{x} \in \mathcal{L} : x_k > 0\}$. Thanks to the homogeneity of $\mathbf{Y}$, we have the stochastic representation

$$\mathbf{Y}^k \stackrel{d}{=} \mathbf{W}^k + E\mathbf{1}, \tag{7}$$

where E has a standard exponential distribution that is independent of a d-variate random vector $\mathbf{W}^k$. The latter is called the kth extremal function, and it satisfies $W_k^k = 0$ almost surely. We refer to Dombry and Eyi-Minko (2013) and Engelke and Hitz (2020) for more background on extremal functions.

Remark 2.1. Multivariate Pareto distributions are often introduced by normalizing the random vector $\mathbf{X}$ to standard Pareto margins (Engelke and Hitz (2020)). As in copulas, this changes only the marginal distributions of $\mathbf{Y}$ but not the extremal dependence structure. Rootzén and Tajvidi (2006) denote multivariate Pareto distributions with general margins as multivariate generalized Pareto distributions, in analogy to the generalized Pareto distributions in the univariate case, which also include exponential distributions. In our paper we opt for the exponential scale since it makes the results more concise. Nevertheless, we say that $\mathbf{Y}$ follows a multivariate Pareto distribution and drop the "generalized" for simplicity.

Many alternative coefficients for extremal dependence have been studied. This includes the madogram (Cooley et al. (2006)) and a coefficient by Larsson and Resnick (2012) used for dimension reduction in Cooley and Thibaud (2019), Fomichov and Ivanovs (2023) and Drees and Sabourin (2021); see the review Engelke and Ivanovs (2021) for details. Another summary statistic introduced in Engelke and Volgushev (2022) is the extremal variogram rooted in $k \in [d]$, which for a multivariate Pareto distribution $\mathbf{Y}$ is

$$\Gamma_{ij}^{(k)} = \text{Var}\big(Y_i^k - Y_j^k\big), \quad i, j \in [d], \tag{8}$$

given that the variance exists.

While summary statistics provide a first idea of the strength of dependence, they are mainly used for exploratory analysis and model assessment. Approaches that study probabilistic properties of the whole distribution are more powerful to improve statistical inference. Examples are the notions of

conditional independence or positive dependence. In Section 3 we, therefore, discuss how positive dependence and, in particular, can be exploited for multivariate Pareto distributions.

2.3. **Hüsler–Reiss distributions.** An important example of a multivariate Pareto distribution is the Hüsler–Reiss distribution, which can be seen as the analogue of the Gaussian distribution inside the class of multivariate Pareto distributions.

For a fixed $d \in \mathbb{N}$, let $\mathbb{S}_0^d$ be the set of symmetric $d \times d$-matrices with zero diagonal. We say that $\Gamma \in \mathbb{S}_0^d$ is a conditionally negative definite matrix if $\boldsymbol{x}^T \Gamma \boldsymbol{x} \leq 0$ for all $\boldsymbol{x} \in \mathbb{R}^d$ such that $\boldsymbol{x}^T \boldsymbol{1} = 0$. Moreover, Γ is strictly conditionally negative definite if the inequality is always strict, unless $\boldsymbol{x} = \boldsymbol{0}$. We denote the cone of such matrices by $\mathcal{C}^d \subset \mathbb{S}_0^d$. In Appendix A we collect various results on such matrices, which will be useful in the next sections. Note that, from here on, we will abbreviate singleton set $\{k\}$ by k and index sets $[d] \setminus k$ by $\setminus k$.

The d-variate Hüsler–Reiss distribution is a multivariate Pareto distribution parametrized by $\Gamma \in \mathcal{C}^d$ (Hüsler and Reiss (1989)). In this case the random vector $\mathbf{W}_{\setminus k}^k$ in (7) has a $(d-1)$-dimensional normal distribution with mean vector $-\operatorname{diag}(\Sigma^{(k)})/2$ and covariance $\Sigma^{(k)}$ obtained from Γ via the covariance mapping

$$(9) \qquad \Sigma_{ij}^{(k)} = \frac{1}{2}(\Gamma_{ik} + \Gamma_{jk} - \Gamma_{ij}), \quad i, j \neq k;$$

see Engelke et al. (2015) for details and Deza and Laurent (1997) for the importance of this mapping in the more general context of distance geometry. Note that (9) is a linear isomorphism from $\mathbb{S}_0^d$ to the space $\mathbb{S}^{d-1}$ of all symmetric $(d-1) \times (d-1)$ matrices and its inverse is given by

$$(10) \qquad \begin{cases} \Gamma_{ik} = \Sigma_{ii}^{(k)}, & i \neq k, \\ \Gamma_{ij} = \Sigma_{ii}^{(k)} + \Sigma_{jj}^{(k)} - 2\Sigma_{ij}^{(k)}, & i, j \neq k. \end{cases}$$

The image of the cone $\mathcal{C}^d$ under the linear mapping (9) is the set of all positive definite matrices in $\mathbb{S}^{d-1}$; for a proof, see Lemma 3 in Engelke and Hitz (2020) or Lemma A.8 in Appendix A. Therefore, $\Sigma^{(k)}$ is positive definite.

Using the standard terminology of exponential families, in the multivariate Gaussian distribution the covariance matrix is the mean parameter, and its inverse is the canonical parameter. Working with the inverse is useful, as the log-likelihood function is a strictly concave function. Analogously, a useful parameterization for the Hüsler–Reiss distribution is discussed in Hentschel et al. (2022). Let $\Theta^{(k)}$ denote the inverse of $\Sigma^{(k)}$. Define the matrix $\Theta \in \mathbb{S}^d$ as

$$(11) \qquad \Theta_{ij} := \Theta_{ij}^{(k)} \quad \text{for some } k \neq i, j.$$

Note that $\Theta_{ij}^{(k)} = \Theta_{ij}^{(k')}$ for $i, j \neq k, k'$ by Engelke and Hitz (2020, Lemma 1). We call Θ the Hüsler–Reiss precision matrix. An important alternative characterization of Θ is obtained as follows. Define the projection matrix

$$(12) \qquad \boldsymbol{P} := I_d - \frac{1}{d}\boldsymbol{1}\boldsymbol{1}^T,$$

and let $\Sigma := \boldsymbol{P}(-\frac{\Gamma}{2})\boldsymbol{P}$. By Lemma A.6 if $\Gamma \in \mathcal{C}^d$, then Σ is positive semidefinite. Moreover, $\operatorname{rank}(\Sigma) = d - 1$ and $\Sigma \boldsymbol{1} = \boldsymbol{0}$. Denote by A^+ the Moore–Penrose pseudoinverse of A.

Proposition 2.2 (Hentschel et al. (2022)). *Consider Θ defined in (11) and Σ as above. We have $\Theta = \Sigma^+$. It follows that $\operatorname{rank}(\Theta) = d - 1$ and $\Theta \boldsymbol{1} = \boldsymbol{0}$.*

The matrix Θ plays a particularly important role in connection with positive dependence. This will be discussed in the Section 3.2.

2.4. **Graphical models for multivariate Pareto distributions.** Let $\mathbf{Y}$ be a multivariate Pareto random vector with support on the space $\mathcal{L}$. As mentioned above, the vector $\mathbf{Y}^k$ is supported on a product space $\mathcal{L}^k$. The construction of $\mathbf{Y}^k$ allows to define extremal conditional independence for multivariate Pareto distributions as follows.

Definition 1 (Engelke and Hitz (2020, Definition 5)). Let A, B, C be disjoint subsets of $[d]$. $\mathbf{Y}_A$ is extremal conditionally independent of $\mathbf{Y}_B$, given $\mathbf{Y}_C$ (abbreviated as $\mathbf{Y}_A \perp_e \mathbf{Y}_B | \mathbf{Y}_C$), if for all $k \in [d]$, it holds that

$$\tag{13} \mathbf{Y}_A^k \perp\!\!\!\perp \mathbf{Y}_B^k | \mathbf{Y}_C^k.$$

It was shown that the condition in Definition 1 can be weakened (Engelke and Hitz, 2020, Proposition 1), and in fact, extremal conditional independence $\mathbf{Y}_A \perp_e \mathbf{Y}_B | \mathbf{Y}_C$ already holds if there exists a $k \in C$ in the conditioning set such that (13) is satisfied.

Probabilistic graphical models encode conditional independence in graph structures. Let $G = (V, E)$ be an undirected graph with vertex set $V = [d]$ and edge set E. A random vector $\mathbf{X}$ satisfies the pairwise Markov property with respect to G, when

$$X_i \perp\!\!\!\perp X_j | \mathbf{X}_{\setminus ij}, \quad \text{if } (i, j) \notin E.$$

In this case we call $\mathbf{X}$ a *probabilistic graphical model*.

Example 2. For a multivariate Gaussian random vector $\mathbf{X}$ with invertible covariance Σ and concentration matrix $K = \Sigma^{-1}$, it holds that $X_i \perp\!\!\!\perp X_j | \mathbf{X}_{\setminus ij}$ if and only if $K_{ij} = 0$. This means that for Gaussian graphical models, the concentration matrix contains the graph structure.

Definition 1 allows us to define graphical models that encode extremal conditional independence. Let $G = (V, E)$ be an undirected graph with vertex set V and edge set E. A multivariate Pareto vector $\mathbf{Y}$ satisfies the pairwise Markov property on $\mathcal{L}$ with respect to G when

$$Y_i \perp_e Y_j | \mathbf{Y}_{\setminus ij} \quad \text{if } (i, j) \notin E.$$

This means that Y_i and Y_j are extremal conditionally independent, given all other variables, if there is no edge between i and j in G. In fact, this resembles probabilistic graphical models, only with extremal conditional independence instead of standard conditional independence. In this case $\mathbf{Y}$ is called an extremal graphical model on G. For a decomposable graph G and if $\mathbf{Y}$ has a positive and continuous density $f_{\mathbf{Y}}$, Engelke and Hitz (2020, Theorem 1) proves a Hammersley–Clifford theorem, showing the equivalence of the pairwise and global Markov properties, as well as a factorization of the density $f_{\mathbf{Y}}$ with respect to G. Note that if $\mathbf{Y}$ has a density, then extremal graphical models are only defined for connected graphs (Engelke and Hitz, 2020, Remark 1), since marginal independence $\mathbf{Y}_A \perp_e \mathbf{Y}_B$, $A, B \subset V$, would contradict the existence of the density. This can be relaxed by dropping the assumption on existence of densities; see Kirstin Strokorb's discussion of Engelke and Hitz (2020).

Example 3. It was shown in Engelke and Hitz (2020, Proposition 3) that extremal conditional independence for Hüsler–Reiss distributions can be read off from the inverse covariance matrix $\Theta^{(k)} := (\Sigma^{(k)})^{-1}$. By construction the extremal conditional independence does not depend on k, and this is also reflected by the relation between the $\Theta^{(k)}$ for different $k \in V$ (Engelke and Hitz, 2020, Lemma 1). Hentschel et al. (2022) uses this to rephrase extremal conditional independence in terms of the Hüsler–Reiss precision matrix Θ in (11) such that

$$\tag{14} Y_i \perp_e Y_j | \mathbf{Y}_{\setminus ij} \quad \Longleftrightarrow \quad \Theta_{ij} = 0.$$

This equivalence shows the strong similarity of Hüsler–Reiss distributions with multivariate Gaussians, where conditional independences can be read off from the precision matrix.

We have seen that the Hüsler–Reiss distribution has many similar properties with respect to extremal conditional independence as the Gaussian distribution with respect to standard conditional independence. It can, therefore, be considered as an analogue of a Gaussian graphical model among extremal graphical models.

3. EXTREMAL MTP$_2$ DISTRIBUTIONS

In this section we introduce a notion of total positivity in extremes. For some of the most popular parametric families, such as Hüsler–Reiss and logistic distributions, we show how this property is characterized.

3.1. **Extremal positivity for multivariate Pareto distributions.** Total positivity in (3) is defined from an inequality where a probability density is evaluated at two points and their corresponding componentwise minimum and maximum. The space $\mathcal{L}$ in the definition of multivariate Pareto distributions is not closed under these componentwise operations. Definition (3) is thus not directly applicable to multivariate Pareto distributions. Similar to extremal conditional independence (see Definition 1), we define the extremal version of MTP$_2$.

Definition 2. Let $\mathbf{Y}$ be a multivariate Pareto random vector. We say that $\mathbf{Y}$ is extremal multivariate totally positive of order 2 (EMTP$_2$) if and only if $\mathbf{Y}^k$ is MTP$_2$ for all $k \in [d]$.

Using the stochastic representation (7), we will rewrite this definition as an explicit condition on the extremal function $\mathbf{W}^k$. This uses the notion of strong MTP$_2$ distributions given in (4) and the following result. Recall that the support of a density function f is the smallest closed set over which the density integrates to 1.

Theorem 3.1. *Let X_0 be a random variable whose density is supported on $[c, \infty)$ for some $c \in \mathbb{R}$, and let $\mathbf{X} = (X_1, \ldots, X_d)$ be a random vector such that $X_0 \perp\!\!\!\perp \mathbf{X}$. Let $\mathbf{Z} = (X_0, \mathbf{X} + X_0 \mathbf{1})$. Then:*

  1. $\mathbf{Z}$ *is* MTP$_2$ $\iff$ $\mathbf{X}$ *is strongly* MTP$_2$.
  2. $\mathbf{Z}$ *is strongly* MTP$_2$ $\iff$ X_0 *and* $\mathbf{X}$ *are strongly* MTP$_2$.

The above theorem provides a fundamental result on positive dependence properties of convolutions of random vectors. We discuss in Section 8 how it can be used in the analysis of general multivariate extreme value models.

In the sequel we concentrate on particular application of this theorem to the representation (7). This gives us a simple way of verifying whether a multivariate Pareto distribution $\mathbf{Y}$ is EMTP$_2$ and shows how the strong MTP$_2$ property becomes important in our setting.

Theorem 3.2. *Let $\mathbf{Y}$ be a multivariate Pareto distribution and $\mathbf{W}^k$ the kth extremal function, as defined in (7). Then $\mathbf{Y}$ is EMTP$_2$ if and only if the distribution of $\mathbf{W}^k_{\setminus k}$ is strongly MTP$_2$ for all $k \in [d]$. Equivalently, $\mathbf{W}^k_{\setminus k}$ is strongly MTP$_2$ for some $k \in [d]$.*

The next result gives a useful property of EMTP$_2$ distributions, in particular, in connection with latent trees models in Section 4.1. Recall the definition of the margins of a multivariate Pareto distribution in Section 2.2.

Proposition 3.3. *If a multivariate Pareto distribution $\mathbf{Y}$ is EMTP$_2$, then for any $I \subset [d]$ the margin $\mathbf{Y}_I$ is also EMTP$_2$.*

3.2. **Hüsler–Reiss distributions.** For the Hüsler–Reiss distribution, the extremal function is distributed according to a degenerate Gaussian distribution. Let Θ be the Hüsler–Reiss precision matrix defined in (11). Denote $\mathbb{U}_+^d \subset \mathbb{S}^d$ to be the set of all graph Laplacians for connected graphs with positive weights on each edge. In other words, $\mathbb{U}_+^d$ is the set of $d \times d$ symmetric matrices with zero row sums and nonpositive off-diagonal entries whose support correspond to a connected graph.

Theorem 3.4. *Suppose* $\mathbf{Y}$ *has Hüsler–Reiss distribution with variogram matrix* Γ. *Then* $\mathbf{Y}$ *is* EMTP$_2$ *if and only if* Θ *is the Laplacian matrix of a* connected *graph with positive edge weights. Other equivalent conditions are:*

- *(i)* $\Theta_{ij} \leq 0$ *for all* $i \neq j$.
- *(ii) For all* $k = 1, \ldots, d$, $\Theta^{(k)}$ *is a diagonally dominant M-matrix.*
- *(iii) For all* $k = 1, \ldots, d$, $\Theta^{(k)}$ *is an M-matrix.*
- *(iv) For some* $k \in [d]$, $\Theta^{(k)}$ *is a diagonally dominant M-matrix.*

Remark 3.5. Note that this theorem and standard results on graph Laplacians imply that every support is possible in Θ as long as it corresponds to a connected graph.

We now discuss the examples of bivariate and trivariate Hüsler–Reiss distributions with respect to Theorem 3.4.

Example 4. The bivariate Hüsler–Reiss distribution is generated from a Gaussian random variable with mean $-\Gamma_{12}/2$ and variance Γ_{12}. Therefore, as $\Theta^{(1)} = \Theta^{(2)} = 1/\Gamma_{12}$ is always positive by definition of Γ_{12}, it is always a diagonally dominant M-matrix, and it follows that the bivariate Hüsler–Reiss distribution is EMTP$_2$ for any Γ_{12}.

Example 5. Let $d = 3$. Then

$$\Theta = \frac{1}{\det(\Sigma^{(k)})} \begin{pmatrix} 2\Gamma_{23} & \Gamma_{12} - \Gamma_{13} - \Gamma_{23} & -\Gamma_{12} + \Gamma_{13} - \Gamma_{23} \\ \Gamma_{12} - \Gamma_{13} - \Gamma_{23} & 2\Gamma_{13} & -\Gamma_{12} - \Gamma_{13} + \Gamma_{23} \\ -\Gamma_{12} + \Gamma_{13} - \Gamma_{23} & -\Gamma_{12} - \Gamma_{13} + \Gamma_{23} & 2\Gamma_{12} \end{pmatrix}.$$

The conditions in Theorem 3.4(ii) translate to the triangle inequalities

$$(15) \qquad \begin{aligned} \Gamma_{12} &\leq \Gamma_{13} + \Gamma_{23}, \\ \Gamma_{13} &\leq \Gamma_{12} + \Gamma_{23}, \\ \Gamma_{23} &\leq \Gamma_{12} + \Gamma_{13}, \end{aligned}$$

where the second and the third inequality come from the row sums. Note the symmetry in the inequalities, as EMTP$_2$ does not depend on k. It follows that for trivariate Hüsler–Reiss distributions, EMTP$_2$ is equivalent to Γ being a metric.

As we remarked in Appendix A.3, as long as Γ is a strictly conditionally negative matrix, $\sqrt{\Gamma_{ij}}$ are always distances in the sense that the map $(i, j) \mapsto \sqrt{\Gamma_{ij}}$ is a metric function (satisfies the triangle inequality). In the special case when Θ is a Laplacian matrix, as in Theorem 3.4, the map $(i, j) \mapsto \Gamma_{ij}$ is also a metric function by Lemma A.11. In the electrical network literature, this corresponds to the statement that if Θ is a Laplacian of a connected graph then the corresponding resistances Γ define a metric (Fiedler (1998); Devriendt (2022); Klein and Randić (1993)). In Example 5 we showed that these two conditions are equivalent if $d = 3$. If $d > 3$, then Γ being a metric is a strictly weaker condition. Here we present a probabilistic interpretation for the case when Γ is a metric. Recall the classical notion of positive association (Esary et al. (1967)): A random vector $\mathbf{X}$ is positively associated if $\text{Cov}(f(\mathbf{X}), g(\mathbf{X})) \geq 0$ for any two nondecreasing functions f, g for which this covariance exists. By Pitt (1982), a Gaussian $\mathbf{X}$ is positively associated if and only if its covariance matrix has only nonnegative entries.

Proposition 3.6. *The parameter matrix Γ in a Hüsler–Reiss random vector satisfies the triangle inequality $\Gamma_{ij} \leq \Gamma_{ik} + \Gamma_{jk}$ for all $i, j, k \in [d]$ if and only if all extremal functions $\mathbf{W}^k$, $k \in [d]$, are positively associated.*

3.3. **Other important constructions.** Another popular construction of multivariate Pareto distributions arises from extremal functions of the form

$$(16) \qquad \mathbf{W}^k = (U_1 - U_k, \ldots, U_d - U_k),$$

for independent $U_1, \ldots, U_d$. Examples include the extremal logistic (Tawn (1990); Dombry et al. (2016)) and the extremal Dirichlet distribution (Coles and Tawn (1991)), which we will discuss below.

Our next result provides a simple way of checking whether such constructions are EMTP_2.

Proposition 3.7. *Consider the multivariate Pareto distribution with stochastic representation (7). Suppose that $W_i^k = U_i - U_k$ for some independent $U_1, \ldots, U_d$ such that U_i has a log-concave distribution for every $i \in [d]$. Then $\mathbf{Y}$ is EMTP_2.*

From Proposition 3.7 it follows that both the extremal logistic and extremal Dirichlet distributions are always EMTP_2.

Example 6 (Extremal logistic distribution). The extremal logistic distribution with parameter $\theta \in (0, 1)$ is defined by an extremal function $\mathbf{W}^k$, as in (16), with $U_i \sim \mathrm{Gumbel}(\mathrm{location} = \theta G(1 - \theta), \mathrm{scale} = \theta)$ for $i \neq k$ and $(G(1 - \theta) \exp(U_k))^{-1/\theta} := Z \sim \mathrm{Gamma}(\mathrm{shape} = 1 - \theta, \mathrm{scale} = 1)$, where $G(x)$ is the Gamma function (Dombry et al. (2016)). For $i \neq k$, U_i follows a Gumbel distribution, which is log-concave. For $i = k$, observe

$$-U_k = \theta \log(Z) + \log\big(G(1 - \theta)\big),$$

which means that $-U_k \sim \mathrm{ExpGamma}[\mathrm{shape} = 1 - \theta, \mathrm{scale} = \theta, \mathrm{location} = \log(G(1 - \theta))]$ follows an exponential Gamma distribution. An $\mathrm{ExpGamma}[\mathrm{shape} = \kappa, \mathrm{scale} = \theta, \mathrm{location} = \mu]$ distribution has density

$$\frac{1}{\theta G(\kappa)} \exp\left(\frac{\kappa(x - \mu)}{\theta} - \exp\left(\frac{x - \mu}{\theta} \right) \right),$$

which is log-concave. Hence, U_k is log-concave by symmetry. By Proposition 3.7 this implies EMTP_2.

Example 7 (Extremal Dirichlet distribution). The extremal Dirichlet distribution with parameters $\alpha_1, \ldots, \alpha_d$ has an extremal function, as in (16), where $\exp(U_i) \sim \mathrm{Gamma}(\mathrm{shape} = \alpha_i, \mathrm{scale} = 1/\alpha_i)$ for $i \neq k$ and $\exp(U_k) \sim \mathrm{Gamma}(\mathrm{shape} = \alpha_k + 1, \mathrm{scale} = 1/\alpha_k)$ (Engelke and Volgushev (2022)). As the exponential Gamma distribution is log-concave, this is EMTP_2 by Proposition 3.7.

3.4. **Bivariate Pareto distributions and** EMTP_2. A bivariate Pareto distribution $\mathbf{Y} = (Y_1, Y_2)$ is completely characterized by a univariate distribution. Indeed, the extremal function then satisfies $\mathbf{W}^1 = (0, W_2^1)$ with a real-valued random variable W_2^1 with $\mathbb{E}(\exp W_2^1) = 1$. The second extremal function $\mathbf{W}^2 = (W_1^2, 0)$ is determined by the first one through the duality $\mathbb{P}(W_1^2 \leq z) = \mathbb{E}(\mathbb{1}_{\{W_2^1 \geq -z\}} \exp W_2^1)$, $z \in \mathbb{R}$ (Engelke and Hitz, 2020, Example 3). Conversely, any random variable W_2^1 with $\mathbb{E}(\exp W_2^1) = 1$ defines a unique bivariate Pareto distribution through the extremal function and duality.

These results extend to extremal tree models since they are a composition of bivariate Pareto distributions (Engelke and Volgushev (2022)); see Section 4.1 below.

By Theorem 3.2 EMTP_2 is equivalent to the univariate random variable W_2^1 being strongly MTP_2. This gives us the following result.

Theorem 3.8. *A bivariate Pareto distribution is EMTP_2 if and only if the distribution of W_2^1 is log-concave.*

Log-concave distributions include many known families like Gaussian, exponential, uniform, beta or Laplace, but also the class of generalized extreme value distributions such that many bivariate Pareto distributions are indeed EMTP_2 for any parameter. The construction of an example where the bivariate Pareto distribution is not EMTP_2 requires a positive random variable W_2^1 with $\mathbb{E}(\exp W_2^1) = 1$ for which W_1^2 is not log-concave. One example is when $\exp(W_2^1)$ is folded Laplace.

Example 8. Let $\exp(W_2^1) = |X|$, where X is distributed according to a Laplace distribution with mean μ and scale parameter σ. The density of $\exp(W_2^1)$ equals

$$f(y) = \frac{1}{\sigma} \begin{cases} e^{-\mu/\sigma} \cosh(y/\sigma) & \text{for } 0 \le y < \mu, \\ e^{-y/\sigma} \cosh(\mu/\sigma) & \text{for } 0 \le \mu \le y; \end{cases}$$

see also Liu and Kozubowski (2015). The density of W_2^1 equals $e^y f(e^y)$, such that log-concavity of W_2^1 requires that the second derivative of this is nonpositive. We compute for $0 \le y < \mu$

$$\frac{\partial^2}{\partial y^2}\left(y - \log(\sigma) - \frac{\mu}{\sigma} + \log \cosh\left(\frac{e^y}{\sigma}\right)\right) = \frac{\partial^2}{\partial y^2} \log \cosh\left(\frac{e^y}{\sigma}\right)$$
$$= \frac{e^y(\sigma \tanh(\frac{e^y}{\sigma}) + e^y \operatorname{sech}^2(\frac{e^y}{\sigma}))}{\sigma^2},$$

which is clearly positive.

4. EMTP_2 IN GRAPHICAL EXTREMES

The previous section introduced the notion of EMTP_2. In this section we study EMTP_2 in the context of extremal graphical models. We focus on two aspects that we find particularly important. We first discuss the case of extremal tree models and their latent counterparts, which provide another strong theoretical argument for the usefulness of the EMTP_2 constraint. We then characterize extremal conditional independence structures that may appear in EMTP_2 distributions.

4.1. **Extremal tree models.** For any undirected tree $T = (V, E)$, a multivariate Pareto distribution **Y** that is Markov to T is called an extremal tree model (Engelke and Hitz (2020)). Such models also arise as the limits of regularly varying Markov trees (Segers (2020)). Define a directed tree $T^k = (V, E^k)$ rooted in k by directing all edges in T away from k. By Engelke and Volgushev (2022, Proposition 1), for any $k \in V$, the extremal function $\mathbf{W}^k$ has the stochastic representation

$$(17) \qquad W_i^k = \sum_{e \in \mathrm{ph}(ki;T^k)} W_e,$$

where $\mathrm{ph}(ki; T^k)$ is the set of directed edges on the path from k to i in T^k and $\{W_e, e \in E^k\}$ is a set of independent random variables, where W_e with $e = (i, j)$ has the distribution of W_j^i, that is, the jth component of the ith extremal function of **Y**.

For a Hüssler–Reiss tree model on the tree T, it was shown in Engelke and Volgushev (2022, Proposition 4) that the extremal variogram defined in (8) is a tree metric, that is,

$$\Gamma_{ij}^{(k)} = \sum_{mn \in \mathrm{ph}(ij;T)} \Gamma_{mn}^{(k)}.$$

As a consequence, the minimum spanning tree with weights $\Gamma_{ij}^{(k)} > 0$ is unique and equals the underlying tree T (Engelke and Volgushev, 2022, Corollary 1). The link of this model class to Brownian motion tree models is established in Proposition A.12 in Appendix A.

Proposition 4.1. *Extremal tree models are* EMTP_2 *if and only if all bivariate margins are* EMTP_2, *that is, if all* W_e *in* (17) *have log-concave densities. This implies that Hüsler–Reiss tree models are always* EMTP_2.

In comparison, Gaussian tree models are MTP_2 if and only if their covariance is nonnegative (Lauritzen et al., 2019, Proposition 5.3). This is one way to illustrate why EMTP_2 constraints are more natural for extreme data than MTP_2 constraints are in the classical case.

A generalization of an extremal tree model is an extremal *latent* tree model. The latter is defined as a multivariate Pareto distribution $\mathbf{Y}$ obtained as the margin $\tilde{\mathbf{Y}}_O$ of a larger extremal tree model $(\tilde{\mathbf{Y}}_O, \tilde{\mathbf{Y}}_U)$, where $\tilde{\mathbf{Y}}_O$ and $\tilde{\mathbf{Y}}_U$ correspond to the observed and unobserved variables, respectively. Extremal latent tree models have been used in Asenova et al. (2021) for modeling floods on a river network. By Proposition 3.3 every margin of an EMTP_2 distribution is EMTP_2. This implies that every extremal latent tree model is EMTP_2.

We note that the family of latent extremal tree models is much larger than the family of extremal tree models and contains an extremal version of the widely used one-factor model; see Zwiernik (2018) for more examples and basic overview of latent tree models.

Example 9 (Hüsler–Reiss one-factor model). Define an extremal one-factor model as the margin of an extremal tree model over a tree with a single inner node and all other vertices connected to it. Here the margin is taken over the outer nodes. Consider a d-dimensional Hüsler–Reiss vector $\mathbf{Y}$ with parameter matrix Γ with the following form. For a vector $\boldsymbol{a} = (a_1, \ldots, a_d)$ with strictly positive entries, suppose that $\Gamma_{ij} = a_i + a_j$ for all $i \neq j$, $i, j \in [d]$. This is an extremal latent tree model since $\mathbf{Y}$ is the margin of a $(d+1)$-dimensional Hüsler–Reiss tree model on the star tree, where the d leaves correspond to the observed variables and the central node is the unobserved variable; this can be seen since the extended Γ with $\Gamma_{i(d+1)} = a_i$ is a tree metric on the star tree (Engelke and Volgushev (2022), Proposition 4). Using the covariance mapping (9), we see that, for every $i, j, k \in [d]$ with $i, j \neq k$,

$$\Sigma_{ij}^{(k)} = \begin{cases} a_k & \text{if } i \neq j, \\ a_i + a_k & \text{if } i = j. \end{cases}$$

Carefully applying the Sherman–Morrison formula (Horn and Johnson (2013), Section 0.7.4), we see that, for all $i \neq j$,

$$\Theta_{ij} = -\frac{\prod_{l \neq i,j} a_l}{\sum_{k=1}^{d} \prod_{l \neq k} a_l} < 0,$$

which reconfirms that Hüsler–Reiss one-factor models are EMTP_2.

4.2. **Axioms for conditional independence and faithfulness.** Conditional independence models can be discussed in a purely combinatorial way. We follow the definitions in Fallat et al. (2017, Section 5). Let $\langle A, B | C \rangle$ be a ternary relation encoding abstract independence of A and B conditioning on C, where A, B, C are disjoint subsets of V. Here and in the following, unions $A \cup B$ of two sets A, B are abbreviated to AB. A conditional independence model $\mathcal{I}$ is a set of such relations. $\mathcal{I}$ is called a graphoid if it satisfies the following axioms for disjoint $A, B, C, D \subset V$:

1. $\langle A, B | C \rangle \in \mathcal{I} \Leftrightarrow \langle B, A | C \rangle \in \mathcal{I}$ (symmetry),
2. $\langle A, BD | C \rangle \in \mathcal{I} \Rightarrow \langle A, B | C \rangle \in \mathcal{I} \wedge \langle A, D | C \rangle \in \mathcal{I}$ (decomposition),
3. $\langle A, BD | C \rangle \in \mathcal{I} \Rightarrow \langle A, B | CD \rangle \in \mathcal{I} \wedge \langle A, D | BC \rangle \in \mathcal{I}$ (weak union),
4. $\langle A, B | CD \rangle \in \mathcal{I} \wedge \langle A, D | C \rangle \in \mathcal{I} \Leftrightarrow \langle A, BD | C \rangle \in \mathcal{I}$ (contraction),
5. $\langle A, B | CD \rangle \in \mathcal{I} \wedge \langle A, C | BD \rangle \in \mathcal{I} \Rightarrow \langle A, BC | D \rangle \in \mathcal{I}$ (intersection).

A stochastic conditional independence model on a set of distributions is always a semigraphoid, that is, it satisfies axioms (1)–(4). If in addition the distributions have positive densities, then

it is a graphoid. In the discussion of Engelke and Hitz (2020), Steffen Lauritzen discusses that extremal conditional independence models are also semigraphoids. Under the assumption of a positive density $f_{\mathbf{Y}}$, the intersection axiom for extremal conditional independence for multivariate Pareto distributions follows from the fact that then, for any $k \in V$, $\mathbf{Y}^k$ satisfies the intersection axiom for classical stochastic conditional independence because its density is proportional to $f_{\mathbf{Y}}$; see Pearl (2009, Section 1.1.5) or Lauritzen (1996, Proposition 3.1).

For classical conditional independence, if the distributions are MTP$_2$, then Fallat et al. (2017) show that the following additional axioms are satisfied:

(6) $\langle A, B|C \rangle \in \mathcal{I} \wedge \langle A, D|C \rangle \in \mathcal{I} \Rightarrow \langle A, BD|C \rangle \in \mathcal{I}$ (composition),

(7) $\langle i, j|C \rangle \in \mathcal{I} \wedge \langle i, j|lC \rangle \in \mathcal{I} \Rightarrow \langle i, l|C \rangle \in \mathcal{I} \vee \langle j, l|C \rangle \in \mathcal{I}$ (singleton-transitivity),

(8) $\langle A, B|C \rangle \in \mathcal{I} \wedge D \subseteq V \setminus AB \Rightarrow \langle A, B|CD \rangle \in \mathcal{I}$ (upward-stability).

As a consequence, these axioms also hold for extremal conditional independence when the multivariate Pareto distribution is EMTP$_2$. In summary, we have the following theorem.

Theorem 4.2. *Extremal conditional independence for a multivariate Pareto distribution with positive density is a graphoid. If in addition the distribution is* EMTP$_2$*, then it is also upward-stable, singleton-transitive and compositional.*

We omit the proof since the statements follows from the corresponding statements for $\mathbf{Y}^k$, $k \in V$. For extremal conditional independence on multivariate Pareto distributions with positive density, we note that the following peculiarity arises. For instance, for $D = \emptyset$, the right-hand side of Axiom (5) would lead to unconditional independence $A \perp_e BC$, which is impossible, as discussed in Section 2.4. This is not a contradiction to the validity of Axiom (5), since it can be shown that in that case also the left-hand side can not arise.

Remark 4.3. Similar to conditional independence, extremal conditional independence under EMTP$_2$ is equivalent to the respective collection of singleton conditional independences,

$$\mathbf{Y}_A \perp_e \mathbf{Y}_B | \mathbf{Y}_C \quad \Leftrightarrow \quad Y_i \perp_e Y_j | \mathbf{Y}_C \quad \forall i \in A, j \in B.$$

This follows as in Lauritzen and Sadeghi (2018, Corollary 1).

Many constraint-based structure learning algorithms, like the PC algorithm (Spirtes et al. (2000)) that is used to learn the skeleton in directed acyclic graphs, rely on the assumption that the dependence structure in the data-generating distribution reflects faithfully the graph. A distribution in a graphical model over a graph G is faithful if and only each conditional independence corresponds exactly to graph separation. We define extremal faithfulness analogously.

For an undirected graph $G = (V, E)$, we can define an independence model $\mathcal{I}(G)$ through graph separation with respect to G by

$$\langle A, B|C \rangle \in \mathcal{I}(G) \quad \Longleftrightarrow \quad C \text{ separates } A \text{ from } B,$$

where the latter means that all paths on G between A and B cross C. On the other hand, we can introduce an independence model $\mathcal{I}_e(\mathbb{P}_{\mathbf{Y}})$ for a multivariate Pareto distributions $\mathbf{Y}$ through

$$\langle A, B|C \rangle \in \mathcal{I}_e(\mathbb{P}_{\mathbf{Y}}) \quad \Longleftrightarrow \quad \mathbf{Y}_A \perp_e \mathbf{Y}_B | \mathbf{Y}_C.$$

We further define the extremal pairwise independence graph $G_e(\mathbb{P}_{\mathbf{Y}})$ such that

$$(i, j) \in E \quad \Longleftrightarrow \quad \langle i, j|V \setminus \{i, j\} \rangle \in \mathcal{I}_e(\mathbb{P}_{\mathbf{Y}}).$$

A multivariate Pareto distribution $\mathbb{P}_{\mathbf{Y}}$ is said to be extremal faithful to a graph G, if $\mathcal{I}_e(\mathbb{P}_{\mathbf{Y}}) = \mathcal{I}(G)$.

Theorem 4.4. *Let $\mathbf{Y}$ be a multivariate Pareto distribution with positive and continuous density. If $\mathbf{Y}$ is in addition* EMTP$_2$*, then $\mathcal{I}_e(\mathbb{P}_{\mathbf{Y}}) = \mathcal{I}(G_e(\mathbb{P}_{\mathbf{Y}}))$; that is, $\mathbb{P}_{\mathbf{Y}}$ is extremal faithful to its pairwise independence graph.*

The proof is similar to Fallat et al. (2017, Theorem 6.1) who show that stochastic independence models that are MTP$_2$ and satisfy the intersection axiom are always faithful to the corresponding pairwise independence graph. It is available in Appendix C.9.

5. LEARNING TOTALLY POSITIVE HÜSLER–REISS DISTRIBUTIONS

The work of Slawski and Hein (2015) and Lauritzen et al. (2019) show that, in the Gaussian case, the MLE under MTP$_2$ has many nice properties. For example, the maximum likelihood estimator exists with probability 1 as long as the sample size is at least two and the MTP$_2$ constraint works as an implicit regularizer. In this section we study the estimation of Hüsler–Reiss distributions under the EMTP$_2$ constraint replacing the likelihood function with a surrogate likelihood.

5.1. **Surrogate likelihood and its dual.** In order to use properties of Gaussian maximum likelihood theory, we apply a transformation to a Hüsler–Reiss Pareto distribution $\mathbf{Y}$. Recall that $\mathbf{Y}^k$ is defined as the conditioned random vector $\mathbf{Y}|\{Y_k > 0\}$ and that from Section 2.3 we have for a Hüsler–Reiss distribution with parameter matrix $\Gamma \in \mathcal{C}^d$

$$(18) \qquad \left(Y_i^k - Y_k^k\right)_{i \neq k} = \mathbf{W}_{\backslash k}^k \sim N\left(-\operatorname{diag}\left(\Sigma^{(k)}\right)/2, \Sigma^{(k)}\right).$$

Consider a data matrix $y \in \mathbb{R}^{n \times d}$ of n independent observations of $\mathbf{Y}$ with ith row $(y_{i1}, \ldots, y_{id})$. Let $\mathcal{I}_k = \{i \in [n] : y_{ik} > 0\}$ be the index set of observations where the kth coordinate exceeds zero. If $|\mathcal{I}_k| \geq 2$, for any $i \in \mathcal{I}_k$, $k \in [d]$, we define independent observations $\boldsymbol{w}_i$ of $\mathbf{W}^k$ by

$$w_{ij} = y_{ij} - y_{ik}, \quad j = 1, \ldots, d,$$

and let the corresponding sample covariance matrix be

$$(19) \qquad \Omega^{(k)} = \frac{1}{|\mathcal{I}_k|} \sum_{i \in \mathcal{I}_k} (\boldsymbol{w}_i - \bar{\boldsymbol{w}})(\boldsymbol{w}_i - \bar{\boldsymbol{w}})^T \quad \text{where } \bar{\boldsymbol{w}} = \frac{1}{|\mathcal{I}_k|} \sum_{i \in \mathcal{I}_k} \boldsymbol{w}_i.$$

Note that, by construction, $w_{ik} = 0$ for all $i \in \mathcal{I}_k$, and so the kth row/column of $\Omega^{(k)}$ is zero. If $|\mathcal{I}_k| < 2$, set $\Omega^{(k)} = 0$. We obtain the empirical variogram $\bar{\Gamma}^{(k)}$ from $\Omega^{(k)}$ via the inverse covariance mapping

$$(20) \qquad \bar{\Gamma}_{ij}^{(k)} = \Omega_{ii}^{(k)} + \Omega_{jj}^{(k)} - 2\Omega_{ij}^{(k)} \quad \text{for all } i, j.$$

Because the index set $\mathcal{I}_k$ depends on k, the estimator $\bar{\Gamma}^{(k)}$ also depends on k. In order to obtain an estimate of Γ that is symmetric and uses all data, we define the combined empirical variogram as

$$(21) \qquad \overline{\Gamma} := \frac{1}{d} \sum_{k=1}^{d} \bar{\Gamma}^{(k)};$$

see also Engelke and Volgushev (2022, Corollary 2). For each $k = 1, \ldots, d$, via the covariance mapping (9), we obtain an empirical covariance $S^{(k)}$ from $\overline{\Gamma}$.

The inverse covariance matrix of $\mathbf{W}_{\backslash k}^k$ can be estimated by maximizing the surrogate log-likelihood that takes the form

$$(22) \qquad \ell\left(\Theta^{(k)}; S^{(k)}\right) := \log \det \Theta^{(k)} - \operatorname{tr}\left(S^{(k)}\Theta^{(k)}\right),$$

which is derived from (18) by dropping the likelihood contribution of the mean vector $-\operatorname{diag}(\Sigma^{(k)})/2$. Maximizing this would result in an estimate $\widehat{\Theta}^{(k)}$ of $\Theta^{(k)}$ that is close to the maximum likelihood estimator since the mean vector only contains information on the diagonal of $\Sigma^{(k)}$. Note that the function $\ell(\Theta^{(k)}; S^{(k)})$ in (22) is directly related to the log-determinantal Bregman divergence (e.g., Ravikumar et al. (2011)), so its use can be justified outside of the Gaussian setting.

A more elegant formulation of the surrogate log-likelihood that is independent of k is given next. For a square matrix A, denote by $\mathrm{Det}(A)$ its pseudo-determinant, that is, the product of all nonzero eigenvalues. For $\Theta \in \mathbb{S}^d$ with $\Theta \mathbf{1} = \mathbf{0}$ and $Q_{ij} := -\Theta_{ij}$, $i \neq j$, the weighted matrix-tree theorem (Duval et al. (2009)) yields for any $k \in [d]$ that

$$(23) \qquad \mathrm{Det}(\Theta) = d \cdot \det\left(\Theta^{(k)}\right) = d \cdot \sum_{T \in \mathcal{T}} \prod_{ij \in T} Q_{ij},$$

where $\mathcal{T}$ is the set of all spanning trees over the complete graph with vertices $\{1, \ldots, d\}$.

As in Appendix A, we equip $\mathbb{S}_0^d$ with the inner product $\langle\!\langle A, B \rangle\!\rangle := \sum_{i<j} A_{ij} B_{ij}$.

Lemma 5.1. *The right-hand side of* (22) *can be rewritten in terms of* Θ *as*

$$(24) \qquad \ell(\Theta; S) = \log \mathrm{Det}\, \Theta - \langle S, \Theta \rangle - \log(d),$$

where $S = \boldsymbol{P}(-\frac{1}{2}\overline{\Gamma})\boldsymbol{P}$ *with* $\boldsymbol{P}$ *defined in* (12) *or, equivalently, in terms of* $Q \in \mathbb{S}_0^d$ *as*

$$(25) \qquad \ell(Q; \overline{\Gamma}) = \log\left(\sum_{T \in \mathcal{T}} \prod_{ij \in T} Q_{ij}\right) - \langle\!\langle \overline{\Gamma}, Q \rangle\!\rangle.$$

Note that it follows from (25) that a proportional representation of the log-likelihood in terms of Θ and $\overline{\Gamma}$ is given by (1).

In order to enforce the EMTP$_2$ constraint for the Hüsler–Reiss distribution, we propose to solve a restricted optimization problem using the characterization in Theorem 3.4. Recall that $\mathbb{U}_+^d \subset \mathbb{S}^d$ denotes the set of all graph Laplacians for connected graphs with positive weights on each edge. Slightly abusing notation, we also denote by $\mathbb{U}_+$ its image in $\mathbb{S}_0$, that is, the points in the nonnegative orthant of $\mathbb{S}_0$ whose support is a connected graph. Thus, for any fixed $\overline{\Gamma}$ we consider the problem of maximizing $\ell(Q; \overline{\Gamma})$ in (25) over $\mathbb{U}_+$, that is,

$$(26) \qquad \widehat{Q} := \arg\max_{Q \in \mathbb{U}_+} \ell(Q; \overline{\Gamma}).$$

This is a convex optimization problem because $\ell(Q; \overline{\Gamma})$ is a strictly concave function over the convex set $\mathbb{U}_+$.

We call $\widehat{Q}$ a surrogate maximum likelihood estimator for Q under EMTP$_2$. To obtain an estimator $\widehat{\Gamma}$ for the variogram under EMTP$_2$, we first take $\widehat{\Theta}$, given by $\widehat{\Theta}_{ij} = -\widehat{Q}_{ij}$, to define $\widehat{\Sigma} = \widehat{\Theta}^+$ and then map

$$\widehat{\Gamma}_{ij} = \widehat{\Sigma}_{ii} + \widehat{\Sigma}_{jj} - 2\widehat{\Sigma}_{ij},$$

as explained in Appendix A. This is not the maximum likelihood estimator of Γ under the EMTP$_2$ constraint because we have dropped the contribution of the mean vector as in (22). Nevertheless, $\widehat{\Gamma}$ is a very natural estimator since it has a simple interpretation in terms of the input matrix $\overline{\Gamma}$; see Theorem 5.3 below. Moreover, we show in Proposition 5.7 that it is a consistent estimator.

To analyze this optimization problem in more detail, we study it from the perspective of convex analysis. We first derive its dual problem.

Proposition 5.2. *The dual problem of* (26) *is*

$$(27) \qquad \textit{maximize } \log\det\left(\begin{bmatrix} 0 & -\mathbf{1}^T \\ \mathbf{1} & -\frac{1}{2}\Gamma \end{bmatrix}\right) + (d-1) \quad \textit{subject to } \Gamma \in \mathcal{C}^d \textit{ and } \Gamma \leq \overline{\Gamma}.$$

Proof. Let $\mathcal{K}^d$ be the set of all $Q \in \mathbb{S}_0^d$ such that the corresponding Γ lies in $\mathcal{C}^d$. For given $\overline{\Gamma}$ we define the extended-real-valued function

$$(28) \qquad f(Q) = \begin{cases} -\ell(Q; \overline{\Gamma}) & \text{if } Q \in \mathcal{K}^d, \\ +\infty & \text{otherwise.} \end{cases}$$

The problem in (26) can be therefore reformulated as follows:

(29)   minimize $f(Q)$ subject to $Q \geq 0$.

The Lagrangian for this problem is $f(Q) - \langle\langle \Lambda, Q \rangle\rangle$, where $\Lambda \in \mathbb{S}_0^d$ and $\Lambda_{ij} \geq 0$ for all $1 \leq i < j \leq d$ (Lagrange multipliers of the nonnegative constraints). Clearly,

$$\sup_{\Lambda \geq 0}\{f(Q) - \langle\langle \Lambda, Q \rangle\rangle\} = \begin{cases} f(Q) & \text{if } Q \geq 0, \\ +\infty & \text{otherwise.} \end{cases}$$

This implies that Problem (29) is equivalent to

$$\inf_Q \sup_{\Lambda \geq 0}\{f(Q) - \langle\langle \Lambda, Q \rangle\rangle\},$$

where the infimum is unrestricted. By duality theory (Slater's conditions), we obtain the same value by swapping inf and sup. We obtain the Lagrange dual function

$$\inf_Q\{f(Q) - \langle\langle \Lambda, Q \rangle\rangle\}.$$

If the infimum exists, it is obtained at the unique $Q \in \mathcal{K}^d$ for which the gradient of $f(Q) - \langle\langle \Lambda, Q \rangle\rangle$ vanishes. By Proposition A.5

$$\nabla_Q \log\left(\sum_{T \in \mathcal{T}} \prod_{ij \in T} Q_{ij}\right) = \Gamma,$$

and so

$$\nabla\{f(Q) - \langle\langle \Lambda, Q \rangle\rangle\} = -\Gamma + \overline{\Gamma} - \Lambda,$$

showing that the optimal point must satisfy $\Gamma \leq \overline{\Gamma}$ and $\Lambda = \overline{\Gamma} - \Gamma$ and so optimizing the dual function is equivalent to optimizing a function of Γ of the form

(30) $h(\Gamma) = \begin{cases} \log \det\big(\Sigma^{(k)}(\Gamma)\big) + (d-1) & \text{if } \Gamma \leq \overline{\Gamma}, \Gamma \in \mathcal{C}^d, \\ -\infty & \text{otherwise.} \end{cases}$

Finally, we use the Cayley–Menger formula that states that, for every $k = 1, \ldots, d$,

(31) $\det\big(\Sigma^{(k)}\big) = \det\left(\begin{bmatrix} 0 & -\mathbf{1}^T \\ \mathbf{1} & -\frac{1}{2}\Gamma \end{bmatrix}\right).$

$\square$

The proof of the previous result and the KKT conditions imply the following theorem.

Theorem 5.3. *The point $(\widehat{Q}, \widehat{\Gamma})$ is the unique optimal point of $f(Q)$ over $Q \in \mathbb{U}_+$ if and only if:*

   (i) $\widehat{Q}_{ij} \geq 0$ for all $1 \leq i < j \leq d$,
   (ii) $\overline{\Gamma}_{ij} \geq \widehat{\Gamma}_{ij}$ for all $1 \leq i < j \leq d$,
   (iii) $(\overline{\Gamma}_{ij} - \widehat{\Gamma}_{ij})\widehat{Q}_{ij} = 0$ for all $1 \leq i < j \leq d$.

The condition in (iii) implies that the EMTP$_2$ estimator acts as an implicit regularizer since some of the entries of $\widehat{Q}$ will be set to zero. We, therefore, define the EMTP$_2$ graph $\widehat{G} = (V, \widehat{E})$ as the graph with edges

$$(i,j) \notin \widehat{E} \quad \Longleftrightarrow \quad \widehat{Q}_{ij} = 0,$$

which corresponds to the extremal pairwise independence graph of the Hüsler–Reiss distribution with parameter matrix $\widehat{\Gamma}$.

We find as a simple corollary of Theorem 5.3 that the EMTP_2 estimator equals the surrogate maximum likelihood estimator for the graphical model with respect to the estimated EMTP_2 graph $\widehat{G}$.

Corollary 5.4. *Let $\widehat{G} = (V, \widehat{E})$ be the EMTP_2 graph corresponding to $\widehat{Q}$. It follows that the surrogate maximum likelihood estimator of the extremal graphical model with respect to $\widehat{G}$, that is,*

$$\breve{Q} = \operatorname{argmax} \ell(Q; \overline{\Gamma}) \quad \text{subject to } Q_{ij} = 0 \text{ for all } (i,j) \notin \widehat{E}$$

equals the EMTP_2 estimator $\widehat{Q}$.

Proof. It holds from simple derivation and the graphical model constraints that

$$(\breve{\Gamma}_{ij} - \overline{\Gamma}_{ij}) \breve{Q}_{ij} = 0 \tag{32}$$

for all $1 \leq i < j \leq d$. As conditionally negative definite matrix completion is unique (Hentschel et al. (2022)) and (32) is identical to Theorem 5.3(iii), the corollary follows. $\square$

5.2. **Existence of the optimum and its consistency.** Theorem 3.4 and Lemma 5.1 show that optimizing (22) with respect to all diagonally dominant M-matrices $\Theta^{(k)}$ is equivalent to optimizing $-\log \operatorname{Det} \Theta + \langle S, \Theta \rangle$ over all Laplacian matrices Θ of connected graphs, as described in (26). This is precisely the optimization problem considered in equation (3) in Ying et al. (2021). They show in Theorem 1 that the optimum in (26) exists almost surely. The proof of this result in the supplement of Ying et al. (2021) actually reveals a more detailed statement, which is useful for our purposes:

Theorem 5.5. *The optimum of the problem (26) exists if and only if $\overline{\Gamma}_{ij} > 0$ for all $1 \leq i < j \leq d$.*

Note that $\overline{\Gamma}_{ij} = 0$ if and only if $\bar{\Gamma}_{ij}^{(k)} = 0$ for all k; see (21). Moreover, $\bar{\Gamma}_{ij}^{(k)} = 0$ if and only if $\Omega_{ii}^{(k)} = \Omega_{ij}^{(k)} = \Omega_{jj}^{(k)}$. This happens with probability zero with respect to the underlying sample, unless the corresponding index set $\mathcal{I}_k$ satisfies $|\mathcal{I}_k| < 2$. Thus, with probability one, $\overline{\Gamma}_{ij} > 0$, unless for each $k \in [d]$ the event $\{Y_k > 0\}$ is observed at most once in the sample.

We finish this section providing a consistency result that uses consistency of $\overline{\Gamma}$ and the Berge's maximum theorem (see Berge (1997), Section VI.3).

Proposition 5.6. *The function*

$$\overline{\Gamma} \mapsto \widehat{\Gamma} = \operatorname*{argmax}_{\Gamma \in \mathcal{C}^d \cap \{\Gamma \leq \overline{\Gamma}\}} \log \det \left(\begin{bmatrix} 0 & -\mathbf{1}^T \\ \mathbf{1} & -\frac{1}{2}\Gamma \end{bmatrix} \right)$$

is a continuous function over all $\overline{\Gamma}$ such that $\overline{\Gamma}_{ij} > 0$ for all $i \neq j$.

Proof. Consider the function $f : \mathcal{C}^d \to \mathbb{R}$ given by

$$f(\Gamma) := \log \det \left(\begin{bmatrix} 0 & -\mathbf{1}^T \\ \mathbf{1} & -\frac{1}{2}\Gamma \end{bmatrix} \right).$$

This function is indeed well defined by the Cayley–Menger formula in (31) and Lemma A.8 in Appendix A. If $\overline{\Gamma}_{ij} > 0$ for all $i \neq j$, then the set of all $\Gamma \in \mathcal{C}^d$ satisfying $\Gamma \leq \overline{\Gamma}$ (for a fixed $\overline{\Gamma}$) is a bounded nonempty set. Since $\Gamma_{ij} > 0$ for all $i < j$, by Proposition 5.5 there is a unique point in this set that maximizes $f(\Gamma)$, which shows that the arg max mapping in the statement is indeed a well-defined function. Moreover, by strict concavity of $f(\Gamma)$, the same holds if we maximize f over the closure of $\mathcal{C}^d \cap \{\Gamma \leq \overline{\Gamma}\}$. This is a compact set, which we denote by $g(\overline{\Gamma}) := \overline{\mathcal{C}^d} \cap \{\Gamma \leq \overline{\Gamma}\}$, where $\overline{\mathcal{C}^d}$ is the closure of $\mathcal{C}^d$. Consider the set $\mathcal{K}$ of all compact subsets in $\mathbb{S}_0^d$. This set forms a metric space with the Hausdorff distance

$$\mathbb{D}(C, D) := \max \left\{ \max_{\Gamma \in C} d_D(\Gamma), \max_{\Gamma \in D} d_C(\Gamma) \right\}, \quad C, D \in \mathcal{K},$$

where $d_C(\Gamma)$ denotes the Euclidean distance of $\Gamma \in \mathbb{S}_0^d$ to the set $C \in \mathcal{K}$. The mapping $g : \mathbb{S}_0^d \to \mathcal{K}$, defined as above, is a mapping between two metric spaces. This map is continuous if and only if for every sequence if $\Gamma_n \to \overline{\Gamma}$, then $g(\Gamma_n) \to g(\overline{\Gamma})$. Equivalently, we want to show that

$$(33) \qquad \|\Gamma_n - \overline{\Gamma}\| \to 0 \quad \implies \quad \mathbb{D}\big(g(\Gamma_n), g(\overline{\Gamma})\big) \to 0.$$

Let $C_n = g(\Gamma_n)$ and $D = g(\overline{\Gamma})$. Since $\overline{\Gamma}$ is an interior point of $\mathcal{C}^d$, we can assume that $\Gamma_n \in \mathcal{C}^d$ as well. But for every $\Gamma \in \overline{\mathcal{C}^d}$,

$$d_D(\Gamma) = \sqrt{\sum_{i<j} \big(\max\{(\Gamma - \overline{\Gamma})_{ij}, 0\}\big)^2} \leq \sqrt{\sum_{i<j} (\Gamma - \overline{\Gamma})_{ij}^2} = \|\Gamma - \overline{\Gamma}\|.$$

The same argument shows that, for every $\Gamma \in C_n$, we have $d_D(\Gamma) \leq d_D(\Gamma_n)$, and so

$$\max_{\Gamma \in C_n} d_D(\Gamma) = d_D(\Gamma_n) \leq \|\Gamma_n - \overline{\Gamma}\|.$$

By symmetry we can also show that $\max_{\Gamma \in D} d_{C_n}(\Gamma) \leq \|\Gamma_n - \overline{\Gamma}\|$, which implies

$$\mathbb{D}\big(g(\Gamma_n), g(\overline{\Gamma})\big) \leq \|\Gamma_n - \overline{\Gamma}\|$$

and thus also (33). We have established continuity of g. By the maximum theorem in Berge (1997, Section VI.3), the function $\overline{\Gamma} \mapsto \mathrm{argmax}_{\Gamma \in g(\overline{\Gamma})} f(\Gamma)$ is also continuous. $\qquad \square$

As a consequence, we establish the consistency of the estimator $\widehat{\Theta}$ under EMTP_2.

Theorem 5.7. *Let $\mathbf{Y}$ be an EMTP_2 Hüsler–Reiss distribution with parameter matrix Γ. Let $\overline{\Gamma}$ be a consistent estimator of Γ as the sample size $n \to \infty$. Then the EMTP_2 estimator $\widehat{\Gamma}$ based on $\overline{\Gamma}$ is consistent, that is, for any $\varepsilon > 0$,*

$$\mathbb{P}\Big(\max_{i,j \in V} |\widehat{\Gamma}_{ij} - \Gamma_{ij}| > \varepsilon\Big) \to 0, \quad n \to \infty.$$

Proof. Since $\widehat{\Gamma}$ is a continuous function of $\overline{\Gamma}$ by Proposition 5.6, it follows that $\widehat{\Gamma}$ converges in probability to the true Γ by the continuous mapping theorem. $\qquad \square$

Remark 5.8. Engelke and Volgushev (2022, Theorem 1) show that, under certain assumptions, the empirical variogram $\overline{\Gamma}$ is consistent, that is, it converges in probability to the true Γ; see also Section 7.1.

The previous theorem does not imply a consistent recovery of the graph, and in fact, the EMTP_2 algorithm does not directly enforce sparsity. Sparsity is, however, often induced indirectly by the KKT conditions. While it is not expected that the graph structure is recovered in general, one can show that the estimated EMTP_2 graph is with high probability a super-graph of the true underlying structure. In applications this is particularly useful in cases where the estimated EMTP_2 graph, and, therefore, the true underlying graph, is very sparse; see Section 7.2 for an example.

Theorem 5.9. *Let $\mathbf{Y}$ be an EMTP_2 Hüsler–Reiss distribution that is an extremal graphical model on its extremal pairwise independence graph $G = (V, E)$, that is, $\Theta_{ij} = 0$ if and only if $(i, j) \notin E$. Suppose that $\overline{\Gamma}$ is a consistent estimator of Γ as the sample size $n \to \infty$, and let $\widehat{\Gamma}$ be the corresponding EMTP_2 estimator. Then the estimated EMTP_2 graph $\widehat{G} = (V, \widehat{E})$ is asymptotically a super-graph of the true underlying graph G. More precisely,*

$$\mathbb{P}(E \subseteq \widehat{E}) \to 1, \quad n \to \infty.$$

Proof. By Theorem 5.3 (i), it holds that $\widehat{Q} \geq 0$. It follows that

$$\mathbb{P}(E \subseteq \widehat{E}) = \mathbb{P}\big(\forall (i,j) \in E : \widehat{Q}_{ij} > 0\big)$$
$$\geq 1 - \sum_{(i,j) \in E} \mathbb{P}(\widehat{Q}_{ij} = 0).$$

Because $\widehat{\Gamma}$ is consistent by Theorem 5.7, it follows that $\widehat{Q}$ is consistent by the continuous mapping theorem, as the maps from $\widehat{\Gamma}$ to $\hat{\Sigma}^{(k)}$ and $\hat{\Theta}^{(k)}$ to $\widehat{Q}$ are linear and matrix inversion is continuous. Hence, there exists some $\varepsilon > 0$ with

$$\mathbb{P}(\widehat{Q}_{ij} > \varepsilon) \to 1$$

for all $(i,j) \in E$. This implies that the probabilities $\mathbb{P}(\widehat{Q}_{ij} = 0)$ tend to zero, and consequently, $\mathbb{P}(E \subseteq \widehat{E})$ tends to one as $n \to \infty$. $\qquad\square$

Remark 5.10. Even if the distribution of $\overline{\Gamma}$ is asymptotically normal, the distribution of $\widehat{\Theta}$ will be typically intractable. It will be equal to a mixture of projections of the Gaussian distribution on various faces of the polyhedral cone defined by nonnegativity of Q. Even if it was possible to understand this distribution, it would be still hard to handle, as the number of mixture components is exponential in d.

6. An optimization algorithm

Our aim in this section is to develop a numerical algorithm to optimize the surrogate likelihood in (24) in terms of Θ (equiv. (25) in terms of Q). A natural first idea is a projected coordinate descent algorithm, as both the gradient of this function has a simple form and the projection on the set $\Theta \leq 0$ is straightforward. This is precisely the algorithm proposed in Ying et al. (2021). We note, however, that ensuring that at each iteration Θ is a Laplacian of a *connected* graph is harder and it occasionally leads to numerical issues.

In what follows, we develop a block coordinate descent algorithm that optimizes the dual problem updating Γ row by row. This algorithm carefully exploits the structure of the problem and relies on quadratic programming. Although in our setting S that appears in (24) is a positive semidefinite matrix satisfying $S\mathbf{1} = \mathbf{0}$, our algorithm takes as input *any* positive semidefinite matrix satisfying $S_{ii} > 0$ for all $i \in [d]$ and $S_{ij} < \sqrt{S_{ii}S_{jj}}$ for all $i \neq j$. We observe that our algorithm is more stable than the projected gradient descent algorithm in the case when S is rank deficient.

6.1. **General description of the algorithm.** Our algorithm is a block coordinate descent algorithm that optimizes the dual problem (27). We refer to all $\Gamma \in \mathcal{C}^d$ satisfying $\Gamma \leq \overline{\Gamma}$ as the dually feasible points. The algorithm starts at some given dually feasible point, and it updates the Γ matrix row by row. At each step the value of the function increases, and the corresponding point is dually feasible. Updating a row requires solving a quadratic problem. This is similar to the algorithms used for the graphical LASSO (Banerjee et al. (2008); Lauritzen and Zwiernik (2022)) but with important twists.

Denote $A = -\frac{1}{2}\Gamma$, and assume $d \geq 3$. After suitably reordering the rows/columns of A, for any $i = 1, \ldots, d$, we can rewrite the determinant in (27) as

$$(34) \qquad -\det \begin{bmatrix} 0 & 1 & \mathbf{1}^T \\ 1 & 0 & A_{\setminus i,i}^T \\ \mathbf{1} & A_{\setminus i,i} & A_{\setminus i,\setminus i} \end{bmatrix}.$$

The goal in the dual problem (27) is to optimize this expression subject to $\Gamma \leq \overline{\Gamma}$. Instead, we optimize this expression only with respect to $\boldsymbol{y} = A_{\setminus i,i}$. This will lead to a quadratic optimization problem that we can easily solve.

Let $B = (A_{\setminus i, \setminus i})^{-1}$. Since $\Gamma \in \mathcal{C}^d$, also $\Gamma_{\setminus i, \setminus i} \in \mathcal{C}^{d-1}$ and, in particular, $\mathbf{1}^T \Gamma_{\setminus i, \setminus i} \mathbf{1} > 0$. In consequence, by Micchelli (1986, Lemma 3.2) $\Gamma_{\setminus i, \setminus i}$ has $d-2$ negative eigenvalues and one positive eigenvalue. Hence,

$$\det(A_{\setminus i, \setminus i}) = \frac{1}{(-2)^{d-1}} \det(\Gamma_{\setminus i, \setminus i}) < 0.$$

Using the standard Schur complement arguments, (34) can be written as

$$- \det(A_{\setminus i, \setminus i}) \cdot \left(\boldsymbol{y}^T \left(\mathbf{1}^T B \mathbf{1} B - B \mathbf{1} \mathbf{1}^T B \right) \boldsymbol{y} + 2 \mathbf{1}^T B \boldsymbol{y} - 1 \right),$$

which has to be maximized with respect to $\boldsymbol{y}$. Thus, equivalently, to maximize the expression in (34) with respect to $\boldsymbol{y}$, we minimize the quadratic function

$$(35) \qquad \boldsymbol{y}^T \left(B \mathbf{1} \mathbf{1}^T B - \mathbf{1}^T B \mathbf{1} B \right) \boldsymbol{y} - 2 \mathbf{1}^T B \boldsymbol{y},$$

subject to $\boldsymbol{y} \geq -\frac{1}{2} \overline{\Gamma}_{\setminus i, i}$. This is a simple quadratic optimization problem. However, an important complication comes from the fact that the corresponding quadratic form is not positive definite (it contains the vector of ones in its kernel), and so many of the popular quadratic programming algorithms cannot be used. In our calculations we have used the OSQP package in R (Stellato et al. (2020)).

In summary, our algorithm relies on a sequence of simple quadratic optimization problems, and it is outlined below. An implementation of this algorithm is available as the emtp2 function of the R package graphicalExtremes (Engelke et al. (2022)).

The fact that each iteration gives a dually feasible point will be now proven formally.

Proposition 6.1. *Each iteration of Algorithm 1 is a dually feasible point.*

Proof. Since the starting point Γ^0 is an arbitrary dually feasible point, it is enough to show that updating its ith row/column gives a dually feasible point. The constraint $\Gamma \leq \overline{\Gamma}$ is embedded explicitly in the optimization problem, so it is clearly satisfied. To argue that $\Gamma \in \mathcal{C}^d$ (which is not explicitly imposed), note that Γ is obtained by maximizing

$$(36) \qquad \det \left(\begin{bmatrix} 0 & -\mathbf{1}^T \\ \mathbf{1} & -\frac{1}{2} \Gamma \end{bmatrix} \right),$$

which by the Cayley–Menger formula in (31) is equal to the determinant of $\Sigma^{(k)}$ for every $k \in [d]$. Suppose that the algorithm updates the ith row/column of Γ, and fix any $k \neq i$. By Lemma A.8, $\Gamma \in \mathcal{C}^d$ if and only if $\Sigma^{(k)}$ is positive definite. Using Sylvester's criterion, equivalently, $\det(\Sigma_B^{(k)}) > 0$ for every nonempty $B \subseteq [d] \setminus \{i, k\}$ and $B = [d] \setminus \{k\}$ (enough to check the leading principal minors

---

Data: Conditionally negative definite $\overline{\Gamma}$.
Result: A maximizer of (27).
Initialize: $\Gamma = \Gamma^0$ (a dually feasible point, see Section 6.3);
while *there is no convergence* **do**
    for $i = 1, \ldots, d$. **do**
        Update $\Gamma_{i, \setminus i} \leftarrow -2\hat{\boldsymbol{y}}$, where $\hat{\boldsymbol{y}}$ is the minimizer of (35) subject to $\boldsymbol{y} \geq -\frac{1}{2} \overline{\Gamma}_{\setminus i, i}$
    end
end
Algorithm 1: The block coordinate descent algorithm for Hüsler–Reiss distributions under EMTP_2

when the rows of $\Sigma_B^{(k)}$ are arranged so that the ith row/column comes last). By (9), $\Sigma_B^{(k)}$ is an explicit linear function of $\Gamma_{B\cup\{k\}}$. Using the Cayley–Menger formula again, we get

$$(37) \qquad \det\!\left(\Sigma_B^{(k)}\right) = \det\left(\begin{bmatrix} 0 & -\mathbf{1}^T \\ \mathbf{1} & -\frac{1}{2}\Gamma_{B\cup\{k\}} \end{bmatrix}\right).$$

If $B \subseteq [d] \setminus \{i, k\}$, then the update of the algorithm does not affect this quantity, and so $\det(\Sigma_B^{(k)}) > 0$ by the fact that the current estimate was dually feasible. If $B = [d] \setminus \{k\}$, then the right-hand side of (37) becomes (36). This quantity must then be strictly positive after the update because it is at least as big as for the current estimate, which was strictly positive. $\qquad \square$

6.2. **Convergence criteria.** Recall that, by strong duality, we can guarantee that, at the optimal point (Γ^*, Q^*), the value of the primal and the dual functions are equal and for any other point the value of the dual problem is lower. Thus, to obtain a convergence criterion it is natural to track the duality gap

$$(38) \qquad -\log\det\Theta^{(k)} + \langle\!\langle \overline{\Gamma}, Q \rangle\!\rangle - \left(\log\det\Sigma^{(k)} + (d-1)\right) = \langle\!\langle \overline{\Gamma}, Q \rangle\!\rangle - (d-1),$$

which is guaranteed to be always nonnegative and zero precisely at the optimal point. The algorithm may be stopped when the duality gap is lower than some fixed threshold. Optimality of the obtained point can be verified using the KKT conditions in Theorem 5.3. Note, however, that, to compute the duality gap, the current estimate Γ needs to be mapped to Q. This operation involves pseudo-inversion, and so it may be expensive in high-dimensional situations, as the computational complexity of pseudo-inversion is cubic in dimension. In this case we can simply track the absolute change between the updates of Γ, checking the duality gap only in the end to decide if more iterations are needed.

6.3. **A starting point.** For our coordinate descent algorithm to work, we require a feasible starting point. By Proposition 6.1 every subsequent point in our procedure will be dually feasible. Our construction relies on ideas that were used in the context of Gaussian distributions. Let S be a positive semidefinite matrix. By Proposition 3.4 in Lauritzen et al. (2019), as long as $S_{ii} > 0$ for all $i = 1, \ldots, d$ and $S_{ij} < \sqrt{S_{ii}S_{jj}}$ for all $i \neq j$, there exists a positive definite matrix Z such that $Z \geq S$ and Z coincides with S on the diagonal. The construction of such Z links to single-linkage clustering and ultrametrics. Section 3 in Lauritzen et al. (2019) also describes an efficient method for computing Z, which is implemented as function `Zmatrix` in the R package `golazo` (Lauritzen and Zwiernik (2020)). Let Γ^Z be obtained from Z via the inverse covariance mapping. Note that, by construction, Γ^Z is strictly conditionally negative definite and

$$\Gamma_{ij}^Z = Z_{ii} + Z_{jj} - 2Z_{ij} = S_{ii} + S_{jj} - 2Z_{ij} \leq S_{ii} + S_{jj} - 2S_{ij} = \overline{\Gamma}_{ij}.$$

As a consequence, Γ^Z is a valid starting point for our block coordinate descent algorithm.

6.4. **Performance.** In our setup the optimization of (26) arises naturally as the EMTP_2 constraint maximization of the surrogate likelihood of the Hüsler–Reiss distribution. The same optimization problem appears in the literature on graph learning under Laplacian constraints (Egilmez et al. (2017)). While the optimization problem is the same, the way that the input for the algorithm is obtained differs. In our case we estimate the combined empirical variogram $\overline{\Gamma}$ in (21) from samples of the Hüsler–Reiss distribution and derive the matrix S as in Lemma 5.1. In the graph Laplacian learning literature, typically, the matrix S is estimated directly from Gaussian data.

We compare our block coordinate descent algorithm, described in Algorithm 1, with existing methods for numerical optimization of (26). The first method by Egilmez et al. (2017) is the combinatorial graph Laplacian (CGL) algorithm. For the same problem, Zhao et al. (2019) propose an
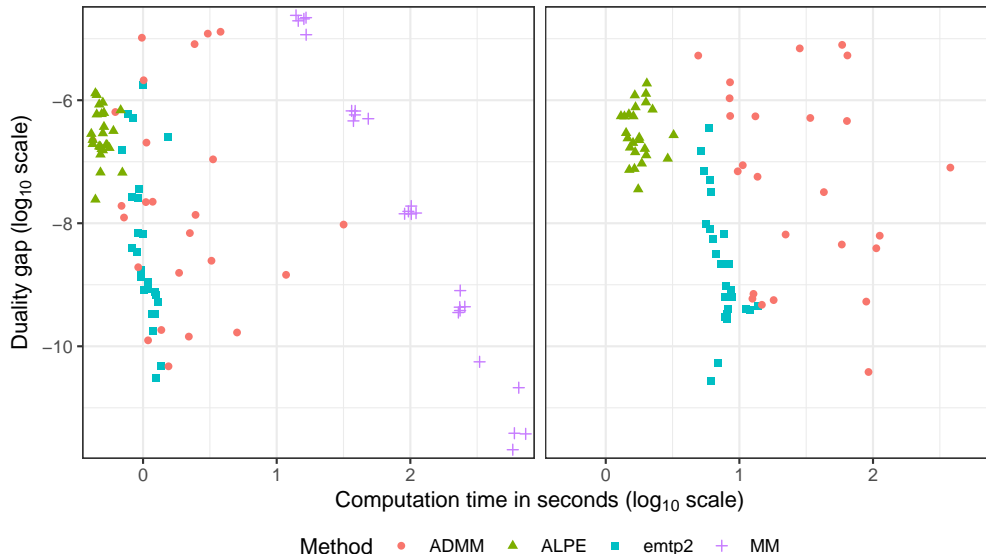
FIGURE 1. Comparison of the algorithms `emtp2`, ADMM, MM and ALPE for $d = 50$ (left) and of the algorithms `emtp2`, ADMM and ALPE for $d = 100$ (right) in terms of computation time and duality gap.

alternating direction method of multipliers (ADMM) and a majorization-minimization (MM) algorithm, whereas Ying et al. (2021) use an adaptive Laplacian constrained precision matrix estimation (ALPE). For the CGL, ADMM and MM algorithms we use the implementations in the R package `spectralGraphTopology` (Vinicius and Palomar (2019)), and for the ALPE method, we use the code from the R package `sparseGraph` (Vinicius et al. (2021)). Since the CGL algorithm did note converge in any of our settings, we do not consider it further.

In order to compare the computation times of the different algorithms and the corresponding precision of the numerical solution, we conduct the following study. We first generate a random variogram matrix Γ as the Euclidean distance matrix of d randomly sampled points from the $(d-1)$-dimensional unit sphere. For a given tolerance, we run each algorithm with input given by this matrix Γ (or the corresponding matrix S). In the first version of this paper, we observed convergence problems for the ALPE and ADMM algorithms in this setting. After contacting the authors of `spectralGraphTopology` and `sparseGraph` and reporting our observations, they kindly provided us with improved versions of their algorithms, adapted to variograms sampled from the Euclidean distances on the $(d-1)$-dimensional ball. Since implementation of the tolerances of the algorithms are not directly comparable, we repeat this procedure several times with different variograms and different tolerances each time.

In the left-hand side of Figure 1, we show the results for $d = 50$ by plotting the duality gap in (38) and the corresponding computation times of the different methods.

We first observe that the adapted ALPE algorithm converges fast, but the duality gap remains between 10^{-6} and 10^{-8}, even when we specify a small tolerance. The ADMM, the MM algorithm and our `emtp2` algorithm achieve similar levels of accuracy, but we see that our algorithm is faster than the ADMM and much faster than the MM algorithm. The right-hand side of Figure 1 shows the same simulation for dimension $d = 100$, where we had to exclude the MM algorithm because of

d	50	100	200	400
computation time	1.00	6.95	70.55	910.76

TABLE 1. Average computation times (in seconds) of our `emtp2` algorithm from 10 simulations for a tolerance of 10^{-5} and different dimensions d.

its huge computation times. Again, we observe that our `emtp2` algorithm is faster than the ADMM algorithm and more accurate than the ALPE algorithm.

We further investigate in Table 1 the computation times of our EMTP_2 algorithm for a range of dimensions d. We observe that, even for higher dimension, the algorithm can be applied in a reasonable time. This may be of interest in applications in high-dimensional statistics where regularization is needed.

All computations in this section were made on a laptop with an Intel Core i5 processor with 1.6 GHz. We note that our vanilla implementation could certainly be largely improved by more efficient programming.

7. APPLICATION

In this section we illustrate the effectiveness of our method by applying it to the extremes of a data set from the Danube River Basin related to flood risk assessment. We also discuss the preprocessing of the data prior to applying our methodology.

7.1. **Data in the domain of attraction.** While in Section 5.1 we assumed to have data points directly from the Hüsler–Reiss distribution $\mathbf{Y}$, in practice, we usually observe data from a nonextreme random vector $\tilde{\mathbf{X}}$ to which we apply a preliminary normalization and thresholding step to select the relevant extremes. Following the theory in Section 2.2, we assume that $\tilde{\mathbf{X}}$ has continuous marginal distribution functions F_j, $j \in [d]$ and define a normalized random vector $\mathbf{X}$ with components

$$(39) \qquad X_j = -\log\big\{1 - F_j(\tilde{X}_j)\big\}, \quad j \in [d]$$

with standard exponential margins. We assume that it is multivariate regularly varying and in the domain of attraction of $\mathbf{Y}$ in the sense of (6). For a data matrix $\tilde{x} \in \mathbb{R}^{m \times d}$ containing m observations of $\tilde{\mathbf{X}}$ in the rows, we obtain a data matrix $x \in \mathbb{R}^{m \times d}$ by applying the transformation (39), with F_j replaced by the empirical distribution functions $\widehat{F}_j$, to the columns of the matrix $\tilde{x}$. The rows of x, denoted by $\mathbf{x}_i$, $i \in [m]$, are approximate observations of $\mathbf{X}$. In a second step, we define the exceedances over some high threshold u as all observations

$$\mathbf{y}_i = \mathbf{x}_i - u\mathbf{1} \quad \text{for all } i \in \mathcal{I} = \big\{l \in [m] : \|\mathbf{x}_l\|_\infty > u\big\},$$

where the number of exceedances $n = |\mathcal{I}|$ depends on the threshold u. If u is sufficiently large, by (6) the vectors $\mathbf{y}_i$, $i \in \mathcal{I}$, are approximate observations of $\mathbf{Y}$. We may now follow the steps in Section 5.1 to compute the combined empirical variogram $\overline{\Gamma}$ based on these data.

Under some regularity conditions, the approximations described above can be made precise to show that the estimator $\overline{\Gamma}$ converges to the true Γ if the number of exceedances satisfies $n \to \infty$ and $n/m \to 0$ (Engelke and Volgushev (2022), Theorem 1). The use of empirical distribution functions for the normalization is standard in multivariate extreme value theory when the focus is on the dependence structure (e.g., Einmahl and Segers (2009); Einmahl et al. (2016)). Similarly to Proposition 5.7, it then directly follows from the continuity of the EMTP_2 algorithm, proved in Proposition 5.6, that the EMTP_2 estimator $\widehat{\Gamma}$ is also consistent for $\overline{\Gamma}$ based on data in the domain of attraction of $\mathbf{Y}$.

7.2. **Danube data.** For an application that is relevant in terms of risk assessment, we consider river discharge data from the Upper Danube Basin, which were originally used in Asadi et al. (2015). The data set consists of daily measurements collected at $d = 31$ gauging stations over 50 years from 1960 to 2009 by the Bavarian Environmental Agency (http://www.gkd.bayern.de). After declustering and selecting only the summer months, Asadi et al. (2015) obtain $m = 428$ observations that are assumed independent. The Danube data are available in the R package `graphicalExtremes` and have been studied in a number of papers with focus on the modeling of extremal dependence (Asadi et al. (2015); Engelke and Hitz (2020)) and detecting the extremal causal structure (Tran et al. (2021); Mhalla et al. (2020); Gnecco et al. (2021)). For more details on the data and the preprocessing, we refer to Asadi et al. (2015). We normalize the data as described in Section 7.1, and, following Engelke and Hitz (2020), we chose the $p = 0.9$ quantile of the marginal Pareto distribution as threshold u, which results in a dataset of $n = 116$ observations.

We begin with an exploratory analysis of the data. From the empirical variogram $\overline{\Gamma}$, we obtain an empirical estimate $\overline{\Theta}$ of the precision matrix. The respective submatrices for the stations $I = \{1, 2, 3, 4, 5\}$ are

$$\overline{\Gamma}_{II} = \begin{pmatrix} 0.00 & 0.53 & 0.65 & 0.73 & 0.82 \\ 0.53 & 0.00 & 0.09 & 0.11 & 0.18 \\ 0.65 & 0.09 & 0.00 & 0.04 & 0.17 \\ 0.73 & 0.11 & 0.04 & 0.00 & 0.15 \\ 0.82 & 0.18 & 0.17 & 0.15 & 0.00 \end{pmatrix},$$

$$\overline{\Theta}_{II} = \begin{pmatrix} 27.24 & -4.65 & 1.69 & 1.01 & -6.32 \\ -4.65 & 50.91 & -18.23 & -8.49 & 0.91 \\ 1.69 & -18.23 & 62.88 & -39.48 & -3.36 \\ 1.01 & -8.49 & -39.48 & 61.91 & -19.37 \\ -6.32 & 0.91 & -3.36 & -19.37 & 78.67 \end{pmatrix}.$$

Considering the full precision matrix, only 250 out of $30 \times 31/2 = 465$ free parameters of $\overline{\Theta}$ are nonpositive, which at first sight seems not to be in line with the assumption of EMTP_2. However, in cases where sparsity is present in data, the true underlying precision matrix Θ contains many zeros, and the corresponding empirical estimates fluctuate around zero. Approximately half of them would, therefore, be positive. If the underlying model is EMTP_2, then the entries of Θ corresponding to edges of the true graph, and likewise, their estimates would be negative. In practice, we do not know the underlying graph, but in the case of the Danube data, there is strong evidence that the true graph contains the flow connection tree (e.g., Engelke and Hitz (2020)). In Figure 2 we, therefore, show boxplots of the entries of the empirical precision matrix $\overline{\Theta}$, grouped by edges that do (left) and do not (right) belong to the flow connection tree. We can see a clear difference that supports the intuition above for underlying EMTP_2 models.

This intuitive reasoning suggests that positive dependence is present in the Danube data. We, therefore, compute our Hüsler–Reiss estimator under the EMTP_2 constraint and denote the resulting variogram and precision matrices by $\widehat{\Gamma}$ and $\widehat{\Theta}$, respectively. To illustrate the regularizing impact of our algorithm, we compare empirical versions estimates above on the subset I of stations to the corresponding EMTP_2 estimates

$$\widehat{\Gamma}_{II} = \begin{pmatrix} 0.00 & 0.53 & \mathbf{0.57} & \mathbf{0.58} & \mathbf{0.60} \\ 0.53 & 0.00 & 0.09 & 0.11 & 0.18 \\ \mathbf{0.57} & 0.09 & 0.00 & 0.04 & \mathbf{0.17} \\ \mathbf{0.58} & 0.11 & 0.04 & 0.00 & 0.15 \\ \mathbf{0.60} & 0.18 & \mathbf{0.17} & 0.15 & 0.00 \end{pmatrix},$$
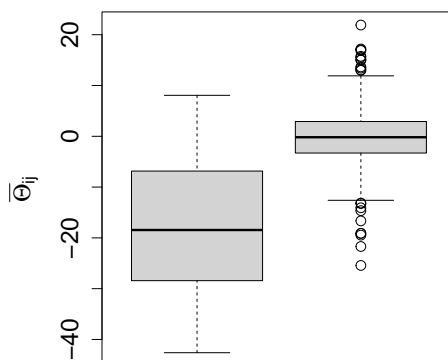
FIGURE 2. Boxplot for empirical estimates $\overline{\Theta}_{ij}$ for edges in the flow graph (left) and the non-diagonal remaining entries (right).

$$\widehat{\Theta}_{II} = \begin{pmatrix} 7.24 & -0.77 & \mathbf{0.00} & \mathbf{0.00} & \mathbf{0.00} \\ -0.77 & 14.16 & -8.79 & -0.53 & -2.06 \\ \mathbf{0.00} & -8.79 & 32.29 & -23.22 & \mathbf{0.00} \\ \mathbf{0.00} & -0.53 & -23.22 & 29.20 & -3.77 \\ \mathbf{0.00} & -2.06 & \mathbf{0.00} & -3.77 & 38.52 \end{pmatrix}.$$

In the matrix $\widehat{\Gamma}_{II}$, we marked in bold the entries that differ from the empirical version $\overline{\Gamma}$; note that $\widehat{\Gamma}_{35}$ begins to differ only in the third decimal. In the submatrix of the precision matrix $\widehat{\Theta}_{II}$, we marked in bold the entries that have been set to zero by the EMTP$_2$ constraint. We observe that these are in correspondence and that in comparison with $\overline{\Gamma}_{II}$, only four out of 10 entries in $\widehat{\Gamma}_{II}$ have changed. This is a consequence of the fact that the EMTP$_2$ solution $(\widehat{\Gamma}, \widehat{\Theta})$ must satisfy the KKT conditions in Theorem 5.3. In particular, Condition (iii) of this theorem imposes zeros in $\widehat{\Theta}$ exactly where $\widehat{\Gamma}$ differs from $\overline{\Gamma}$. By (14) this implies that the Hüsler–Reiss distribution is an extremal graphical model, as defined in Engelke and Hitz (2020), demonstrating how EMTP$_2$ enforces sparsity.

The corresponding extremal graph $\widehat{G} = (V, \widehat{E})$ is shown in the left panel of Figure 3. Interestingly, the EMTP$_2$ graph contains all physical flow connections, with the exception of the edges $(25, 4)$ and $(20, 7)$; see also the geographical map of the Upper Danube Basin in Asadi et al. (2015, Figure 1). Most of the additional connections resemble geographical proximity or similarity, which may corresponds to positive extremal dependence between such nodes. Theorem 5.9 gives us a theoretical foundation to interpret the estimated graph. Indeed, if the model is EMTP$_2$, which is a sensible assumption for the data as argued above, then $\widehat{G}$ asymptotically contains all edges that are present in the true underlying graph G. This means that if an edge is not present in $\widehat{G}$, then it cannot be present in G. Since $\widehat{G}$ is very sparse on this data set, it gives us a good estimate of the extremal graphical model. In particular, it shows that many extremal conditional independences are present between locations that are not neighbors in the flow connection tree.

In order to compare our method to existing approaches, we fit several different Hüsler–Reiss models to the data, some with graphical structure, and some without. The first naive approach is to use the combined extremal variogram $\overline{\Gamma}$, which corresponds to a trivial, fully connected graph. As a simple extremal graphical model based on domain knowledge, we consider a Hüsler–Reiss distribution on the undirected tree given by the physical flow connection of the river network. As an alternative tree model, we fit the minimum spanning tree based on $\overline{\Gamma}$, which is a consistent estimator of the extremal
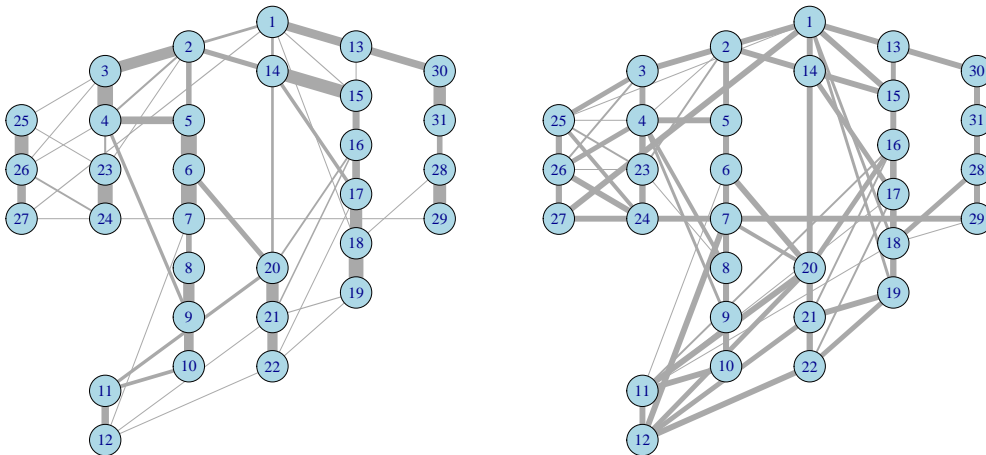
FIGURE 3. Left: Extremal graphical structure of the fitted EMTP_2 Hüsler–Reiss distribution; edge thickness is proportional to $\log(1 - \widehat{\Theta}_{ij})$. Right: Summary of estimated graphical structures of the fitted EMTP_2 Hüsler–Reiss distributions for different thresholds $p \in \{0.7, 0.75, 0.8, 0.85, 0.9, 0.95\}$; edge thickness represents the proportion of occurrences of the edge among the estimated graphs.

graph structure if the true graph is a tree (Engelke and Volgushev (2022)). As discussed in Engelke and Hitz (2020), a tree might be too restrictive, and following their methodology, we fit a sequence of extremal block graph models and choose the best one according to AIC. Asadi et al. (2015) propose a model from spatial extreme value statistics that heavily relies on domain knowledge of this data set, such as catchment sizes and distances between stations. We fit their model in our framework and remark that it has six parameters but corresponds to a fully connected graph. For the sake of fair comparison, we do not use censoring in any of the approaches here (cf., Smith et al. (1997)). For the EMTP_2 estimator, censoring could be achieved by using a censored estimator of Γ in the input of Algorithm 1.

The results of the model fits can be found in Table 2. Among the graphical models, both in terms of AIC and BIC, we observe that our EMTP_2 performs best. This is remarkable since our method does not have any tuning parameters and the assumption of EMTP_2 might seem restrictive. The good performance suggests that the extremes of this data exhibit strong positive dependence, which underlines the theoretical findings of this paper. The spatial model of Asadi et al. (2015) performs similarly to our EMTP_2 estimator in terms of AIC and in terms of BIC, which penalizes the number of model parameters more strongly; the spatial model is first. We note that this comparison is flawed since, as opposed to the spatial model, our estimator is completely data-driven and does not use any domain knowledge. It can, therefore, easily be applied to general multivariate data where no information of the gauging stations is available.

For a sensitivity analysis with respect to the chosen threshold p, we study the estimated EMTP_2 graphs for $p \in \{0.7, 0.75, 0.8, 0.85, 0.9, 0.95\}$. The right panel of Figure 3 shows a summary by a graph with edge width representing the proportion of appearances of the edge among all graphs. We observe that most edges appear in every graph so that the EMTP_2 graph seems to be stable across different threshold choices.

	twice neg logLH	nb par	AIC	BIC
empirical variogram	253.17	465	1183.17	2467.58
flow graph	1447.85	30	1507.85	1590.72
MST	1372.58	30	1432.58	1515.45
best block graph MST	1246.11	42	1330.11	1446.12
Asadi et al.	1090.35	6	1102.35	1118.92
$EMTP_2$ estimator	1017.00	67	1151.00	1336.07

TABLE 2. Results for the different models fitted to the Danube river data set; columns show twice the negative log-likelihood, the number of model parameters and the AIC and BIC values, respectively.

To summarize, the $EMTP_2$ estimator allows for a competitive fit without the choice of tuning parameters and without the need of domain knowledge. In particular, for high-dimensional applications with potentially small sample sizes, our estimator is guaranteed to exist and our algorithm is computationally fast, even for large dimension.

8. DISCUSSION

In this paper we have studied the role of positive dependence in multivariate extreme value theory. In particular, the property of $EMTP_2$ appears naturally in many statistical models and can be characterized by Laplacian precision matrices in the important case of Hüsler–Reiss distributions.

We concentrate on the case of multivariate Pareto distributions, which describe the multivariate tail under asymptotic dependence; see Section 2.2. Our theoretical results rely on the fundamental Theorem 3.1 on the positive dependence of convolutions of a random vectors. In this paper we mainly used this result to link the probabilistic properties of a multivariate Pareto distribution to those of its extremal functions; see Theorem 3.2.

Since the assumptions of Theorem 3.1 are fairly general, it can be applied to a much wider range of models of the form

$$(40) \qquad \widetilde{\mathbf{Z}} = \mathbf{X} + X_0 \mathbf{1},$$

where X_0 is a general random variable, also called common factor, and independent of this, $\mathbf{X}$ is a multivariate random vector. Such models appear as factor models (Lawley and Maxwell (1962); Holland and Rosenbaum (1986)) or random location mixtures in applied probability (Hashorva (2012); Krupskii et al. (2018)).

In the framework of extremes, such location mixtures have been proven to produce versatile tail dependence structures, including both asymptotic dependence and independence (e.g., Engelke et al. (2019)). Intuitively, the heavier the tail of the common factor X_0 relative to the tail heaviness of the components of $\mathbf{X}$, the stronger the dependence of $\widetilde{\mathbf{Z}}$ in the extremes.

A future research direction is to extend the theoretical analysis and statistical methodology of our paper to models for asymptotic independence. Our Theorem 3.1 can be applied to obtain first results. Indeed, as an example, if X_0 has a light tail and $\mathbf{X}$ is multivariate Gaussian, then $\widetilde{\mathbf{Z}}$ is asymptotically independent (Krupskii et al. (2018)), and the strength of residual dependence depends on the correlation matrix of $\mathbf{X}$ (Engelke et al. (2019)). If $\mathbf{X}$ is strongly MTP_2, that is, its precision matrix is a diagonally dominant M-matrix (see Example 1), then Theorem 3.1 implies that $\widetilde{\mathbf{Z}}$ is MTP_2. This theoretical result could be used to regularize such asymptotically independent models by enforcing the MTP_2 constraint.

Another popular approach for asymptotic independence is the model of Heffernan and Tawn (2004). Similar to the definition of $\mathbf{Y}^k$ in (7), this model specifies the multivariate distribution conditional on one variable being extreme. In this case, even though the corresponding model has a form similar to (40), there is dependence between X_0 and $\mathbf{X}$. A different result is, therefore, needed to characterize positive dependence in these models.

Appendix A. The algebra of variogram matrices

A.1. **Algebraic structure.** Let $\mathbb{S}^d$ be the space of real symmetric $d \times d$ matrices and $\mathbb{S}_0^d$ its subspace with zeros on the diagonal. We equip $\mathbb{S}^d$ with the standard trace inner product $\langle A, B \rangle = \text{tr}(AB) = \sum_{i,j} A_{ij} B_{ij}$ and $\mathbb{S}_0^d$ with $\langle\langle A, B \rangle\rangle = \sum_{i<j} A_{ij} B_{ij}$. For $\boldsymbol{b} \in \mathbb{R}^d$ satisfying $\boldsymbol{b}^T \mathbf{1} = 1$, we define:

   (i) linear subspace of $\mathbb{S}^d$: $\mathbb{U}_{\boldsymbol{b}} = \{A \in \mathbb{S}^d : A\boldsymbol{b} = \mathbf{0}\}$,
   (ii) projection on $\mathbb{R}^d/\mathbf{1}$: $\boldsymbol{P}_{\boldsymbol{b}} = I_d - \mathbf{1}\boldsymbol{b}^T$,
   (iii) linear map: $\sigma_{\boldsymbol{b}} : \mathbb{S}_0^d \to \mathbb{U}_{\boldsymbol{b}}$, $A \mapsto \boldsymbol{P}_{\boldsymbol{b}}(-\frac{A}{2})\boldsymbol{P}_{\boldsymbol{b}}^T$.

It is useful to note that, for any $\boldsymbol{a}$, $\boldsymbol{b}$ such that $\boldsymbol{a}^T \mathbf{1} = \boldsymbol{b}^T \mathbf{1} = 1$,

(41) $$\boldsymbol{P}_{\boldsymbol{a}} \boldsymbol{P}_{\boldsymbol{b}} = \boldsymbol{P}_{\boldsymbol{a}}.$$

The relevant cases for us are when $\boldsymbol{b} = \frac{1}{d}\mathbf{1}$ and when $\boldsymbol{b} = \boldsymbol{e}_k$ is a canonical unit vector. If $\boldsymbol{b} = \frac{1}{d}\mathbf{1}$, we omit the subscript writing $\mathbb{U}$ and $\boldsymbol{P}$. In the special case when $\boldsymbol{b} = \boldsymbol{e}_k$, we write $\boldsymbol{P}_k$ and $\mathbb{U}_k$. Note that $\boldsymbol{P}$ is symmetric and it represents the *orthogonal* projection matrix on $\mathbb{R}^d/\mathbf{1}$. Also, $\boldsymbol{P}_k$ has rows $\boldsymbol{e}_i - \boldsymbol{e}_k$, and in particular, the kth row is zero. We denote by $\overline{\boldsymbol{P}}_k \in \mathbb{R}^{(d-1) \times d}$ the matrix obtained from $\boldsymbol{P}_k$ by removing the kth row.

Let $\mathbb{S}_0^d[\Gamma]$, $\mathbb{S}_0^d[Q]$ be two copies of $\mathbb{S}_0^d$ with coordinates denoted by Γ_{ij} and Q_{ij}, respectively. Similarly, we let $\mathbb{U}_{\boldsymbol{b}}[\Sigma]$, $\mathbb{U}_{\boldsymbol{b}}[\Theta]$ be two copies of $\mathbb{U}_{\boldsymbol{b}}$. Consider the following sequence of transformations:

$$\mathbb{S}_0^d[\Gamma] \xrightarrow{\sigma_{\boldsymbol{b}}} \mathbb{U}_{\boldsymbol{b}}[\Sigma] \xrightarrow{\text{ginv}} \mathbb{U}_{\boldsymbol{b}}[\Theta] \xrightarrow{\sigma_{\boldsymbol{b}}^*} \mathbb{S}_0^d[Q],$$

where ginv stands for the generalized inverse $\Sigma \mapsto \Sigma^+$, $\sigma_{\boldsymbol{b}}$ is a linear map defined by $\sigma_{\boldsymbol{b}}(\Gamma) = \boldsymbol{P}_{\boldsymbol{b}}(-\frac{1}{2}\Gamma)\boldsymbol{P}_{\boldsymbol{b}}^T$ and $\sigma_{\boldsymbol{b}}^*$ denotes the adjoint of the linear map $\sigma_{\boldsymbol{b}}$, that is, the unique transformation that satisfies

(42) $$\langle \sigma_{\boldsymbol{b}}(\Gamma), \Theta \rangle = \langle\langle \Gamma, \sigma_{\boldsymbol{b}}^*(\Theta) \rangle\rangle \quad \text{for all } \Gamma \in \mathbb{S}_0^d, \Theta \in \mathbb{U}_{\boldsymbol{b}}.$$

Remark A.1. We note that:

   1. The map $\sigma_{\boldsymbol{b}}$ is invertible with the inverse $\gamma_{\boldsymbol{b}} : \mathbb{U}_{\boldsymbol{b}} \to \mathbb{S}_0^d$, given by

$$\gamma_{\boldsymbol{b}}(\Sigma) = (\Sigma_{ii} + \Sigma_{jj} - 2\Sigma_{ij})_{i<j}.$$

   2. Standard linear algebra gives that the adjoint of the inverse $\gamma_{\boldsymbol{b}}$ is equal to the inverse of the adjoint $\sigma_{\boldsymbol{b}}^*$.
   3. The generalized inverse is a well-defined automorphism on $\mathbb{U}_{\boldsymbol{b}}$.
   4. The inner products are preserved in the sense that, for every $\Gamma, Q \in \mathbb{S}_0^d$ with $\Sigma = \sigma_{\boldsymbol{b}}(\Gamma)$ and $\Theta = \gamma_{\boldsymbol{b}}^*(Q)$, we have that

$$\langle \Sigma, \Theta \rangle = \langle \sigma_{\boldsymbol{b}}(\Gamma), \gamma_{\boldsymbol{b}}^*(Q) \rangle = \langle\langle \gamma_{\boldsymbol{b}}(\sigma_{\boldsymbol{b}}(\Gamma)), Q \rangle\rangle = \langle\langle \Gamma, Q \rangle\rangle.$$

The adjoint map can be easily computed, and its form is particularly simple in the special case when $\boldsymbol{b} = \frac{1}{d}\mathbf{1}$ and when $\boldsymbol{b} = \boldsymbol{e}_k$. To avoid confusion, we introduce different notation for the coordinates of $\mathbb{S}_0^d$ and $\mathbb{U}_{\boldsymbol{b}}$ depending on a particular $\boldsymbol{b}$. We use:

   (i) Σ, Θ to denote coordinates in $\mathbb{U}$,
   (ii) $\widetilde{\Sigma}^{(k)}$, $\widetilde{\Theta}^{(k)}$ to denote coordinates in $\mathbb{U}_k$ and
   (iii) $\Sigma^{(k)}$, $\Theta^{(k)}$ to denote matrices in $\mathbb{S}^{d-1}$ obtained from $\widetilde{\Sigma}^{(k)}$, $\widetilde{\Theta}^{(k)}$ by removing the kth row/column.

Lemma A.2. *The adjoint map $\sigma^* : \mathbb{U}[\Theta] \to \mathbb{S}_0^d[Q]$ is given by $Q_{ij} = -\Theta_{ij}$ for all $1 \le i < j \le d$. The adjoint map $\sigma_k^* : \mathbb{U}_k[\widetilde{\Theta}^{(k)}] \to \mathbb{S}_0^d[Q]$ is given by $Q_{ij} = -\Theta_{ij}^{(k)}$ for all $i, j \neq k$ and $Q_{ik} = \sum_{j \neq k} \Theta_{ij}^{(k)}$.*

Proof. The adjoint maps are defined by (42). We will check this condition on the basis of $\mathbb{S}_0^d$ given by elements of the form $B = E_{ij} + E_{ji}$, where E_{ij} denotes the elementary matrix with the ijth entry equal to one and zero otherwise. Let first $\boldsymbol{b} = \frac{1}{d}\mathbf{1}$. The right-hand side of (42) becomes $(\sigma^*(\Theta))_{ij}$. The left-hand side is

$$\left\langle \boldsymbol{P}\left(-\frac{B}{2}\right)\boldsymbol{P}, \Theta \right\rangle = -\frac{1}{2}\operatorname{tr}(B\boldsymbol{P}\Theta\boldsymbol{P}) = -\frac{1}{2}\operatorname{tr}(B\Theta) = -\Theta_{ij},$$

where we used the fact that $\boldsymbol{P}\Theta\boldsymbol{P} = \Theta$ for all $\Theta \in \mathbb{U}$. The second part of the result follows similar calculations and the fact that $(\boldsymbol{P}_k^T\widetilde{\Theta}^{(k)}\boldsymbol{P}_k)_{ij} = \Theta_{ij}^{(k)}$ if $i, j \neq k$ and $(\boldsymbol{P}_k^T\widetilde{\Theta}^{(k)}\boldsymbol{P}_k)_{ik} = -\sum_{j \neq k}\Theta_{ij}^{(k)}$. $\square$

In our paper we start with the variogram matrix $\Gamma \in \mathbb{S}_0^d$. The matrix $\Sigma^{(k)}$ defined in (9) is a $(d-1) \times (d-1)$ matrix obtained from $\sigma_k(\Gamma) \in \mathbb{U}_k$ by removing the kth row/column. The inverse of σ_k expresses Γ in terms of $\Sigma^{(k)}$ as in (10). The matrix $\Theta = \Sigma^+ = (\boldsymbol{P}(-\frac{1}{2}\Gamma)\boldsymbol{P})^+$ is exactly the same matrix that appears in Proposition 2.2. To easily translate between various equivalent representations of the variogram matrix Γ, we define $f_k : \mathbb{U} \to \mathbb{U}_k$ by $\Sigma \mapsto \boldsymbol{P}_k\Sigma\boldsymbol{P}_k^T$. The following results provides the complete picture of the situation.

Proposition A.3. *The adjoint $f_k^* : \mathbb{U}_k \to \mathbb{U}$ of f_k is defined by $\Theta \mapsto \boldsymbol{P}_k^T\Theta\boldsymbol{P}_k$. Moreover, the following diagram commutes*[1]

$$
\begin{array}{ccccccc}
& & \mathbb{S}^{d-1}[\Sigma^{(k)}] & \xrightarrow{\ \text{inv}\ } & \mathbb{S}^{d-1}[\Theta^{(k)}] & & \\
& & \pi_k \uparrow & & \pi_k^* \downarrow & & \\
\mathbb{S}_0^d[\Gamma] & \xrightarrow{\ \sigma_k\ } & \mathbb{U}_k[\widetilde{\Sigma}^{(k)}] & \xrightarrow{\ \text{ginv}\ } & \mathbb{U}_k[\widetilde{\Theta}^{(k)}] & \xrightarrow{\ \sigma_k^*\ } & \mathbb{S}_0^d[Q] \\
& \searrow\sigma & f_k\uparrow & & f_k^*\downarrow & \nearrow\sigma^* & \\
& & \mathbb{U}[\Sigma] & \xrightarrow{\ \text{ginv}\ } & \mathbb{U}[\Theta] & &
\end{array}
\ ,
$$

where π_k drops the kth row/column of $\widetilde{\Sigma}^{(k)}$ and its adjoint π_k^* embeds $\Theta^{(k)}$ in $\mathbb{U}_k$ by adding the zero row/column. All the maps, apart from the inversion on the top, are well defined everywhere. For the inversion we restrict the map to an open subset where $\Sigma^{(k)}$ is invertible.

Proof. To verify the formula for the adjoint f_k^*, we note that, by definition, it must satisfy

$$\langle f_k(\Sigma), \widetilde{\Theta}^{(k)} \rangle = \langle \Sigma, f_k^*(\widetilde{\Theta}^{(k)}) \rangle \quad \text{for all } \Sigma \in \mathbb{U}, \widetilde{\Theta}^{(k)} \in \mathbb{U}_k,$$

and the formula follows by basic properties of the matrix trace and the fact that $\boldsymbol{P}_{\boldsymbol{b}}^T\widetilde{\Theta}^{(k)}\boldsymbol{P}_{\boldsymbol{b}} \in \mathbb{U}$.

To verify that the diagram commutes, it is enough to check that that it commutes along two side triangles, that is, that $\sigma_k = f_k\sigma$ and $\sigma_k^* = \sigma^*f_k^*$ and along two central rectangles. The bottom rectangle follows by the above calculations. The upper rectangle follows by how pseudoinverse works on the space $\mathbb{U}_k$. To see that $\sigma_k = f_k\sigma$, note that, by (41),

$$f_k(\sigma(\Gamma)) = \boldsymbol{P}_k\boldsymbol{P}\left(-\frac{\Gamma}{2}\right)\boldsymbol{P}\boldsymbol{P}_k^T = \boldsymbol{P}_k\left(-\frac{\Gamma}{2}\right)\boldsymbol{P}_k^T = \sigma_k(\Gamma).$$

To check that $\sigma_k^* = \sigma^*f_k^*$, we use basic properties of the adjoint. $\square$

---

[1]By this we mean that composing maps along any two directed paths with the same beginning and end results in the same function.

Proposition A.3 gives us another way to verify formula (11).

Lemma A.4. *Fix $k \in \{1, \ldots, d\}$ then the form of the mapping f_k^* implies that*

$$\Theta_{ij} = \begin{cases} \Theta_{ij}^{(k)} & \text{if } i, j \neq k, \\ -\sum_{l \neq k} \Theta_{il}^{(k)} & \text{if } i \neq k, j = k, \\ \sum_{i, j \neq k} \Theta_{ij}^{(k)} & \text{if } i = j = k. \end{cases}$$

By Lemma A.2, $\Theta \in \mathbb{U}$ is a weighted Laplacian matrix with potentially negative weights Q_{ij} for $i \neq j$. The weighted matrix-tree theorem used in (23) will be useful for the next result.

Proposition A.5. *The mapping $\mathbb{S}_0^d[\Gamma] \to \mathbb{S}_0^d[Q]$, given by $\Gamma \mapsto \sigma_k^*((\sigma_k(\Gamma))^+)$, is compactly written as*

$$Q = \nabla \log \mathrm{Det}\big(\sigma_k(\Gamma)\big).$$

Similarly,

$$\Gamma = \nabla \log \mathrm{Det}\big(\gamma_k^*(Q)\big).$$

Proof. Let $\overline{\Gamma}$ be a given point in $\mathbb{S}_0^d[\Gamma]$, and let $\widetilde{S}^{(k)} = \sigma_k(\overline{\Gamma}) \in \mathbb{U}_k$. Similarly, let $Q^S = \sigma_k^*((\sigma_k(\overline{\Gamma}))^+)$. By Holbrook (2018),

$$\nabla_\Sigma\big(\log \mathrm{Det}(\Sigma) - \big\langle \Sigma, \big(\widetilde{S}^{(k)}\big)^+ \big\rangle\big)\big|_{\Sigma = \widetilde{S}^{(k)}} = 0.$$

Using the fact that $\sigma_k : \mathbb{S}_0^d \to \mathbb{U}_k$ is an invertible linear mapping, we get that, equivalently,

$$\nabla_\Gamma\big(\log \mathrm{Det}\big(\sigma_k(\Gamma)\big) - \big\langle \sigma_k(\Gamma), \big(\widetilde{S}^{(k)}\big)^+ \big\rangle\big)\big|_{\Gamma = \overline{\Gamma}} = 0.$$

Since $\langle \sigma(\Gamma), (\widetilde{S}^{(k)})^+ \rangle = \langle\!\langle \Gamma, \sigma^*((\widetilde{S}^{(k)})^+) \rangle\!\rangle = \langle\!\langle \Gamma, Q^S \rangle\!\rangle$, we obtain the desired formula. $\qquad\square$

A.2. **Strictly conditionally negative matrices.** The variogram matrices are not only assumed to lie in $\mathbb{S}_0^d$ but they are also assumed to be strictly conditionally negative definite. We study this additional constraint a bit more in this section. Using the notation from Section 2.3, $\Gamma \in \mathcal{C}^d \subset \mathbb{S}_0^d$. In this section we briefly list relevant results that follow from assuming this extra structure.

Remark A.6. If Γ is a conditionally negative definite matrix, then, by the theorem of Schoenberg (Gower (1985); Schoenberg (1935)), equivalently, there exist vectors $\boldsymbol{y}_1, \ldots, \boldsymbol{y}_d$ in some Euclidean space $\mathbb{R}^p$ such that $\Gamma_{ij} = \|\boldsymbol{y}_i - \boldsymbol{y}_j\|^2$. We also call such Γ a Euclidean distance matrix.

Lemma A.7. *If $\Gamma \in \mathcal{C}^d$, then $\Gamma_{ij} > 0$ for all $i \neq j$.*

Proof. Take $\boldsymbol{x} = \boldsymbol{e}_i - \boldsymbol{e}_j$. By definition, $\boldsymbol{x}^T \Gamma \boldsymbol{x} = -2\Gamma_{ij}$ must be strictly negative. $\qquad\square$

Lemma A.8. *The cone $\sigma_{\boldsymbol{b}}(\mathcal{C}^d)$ is precisely the set of all positive semidefinite matrices in $\mathbb{U}_{\boldsymbol{b}}$ of the rank $d-1$. The mapping $\pi_k : \mathbb{U}_k \to \mathbb{S}^{d-1}$ maps $\sigma_k(\mathcal{C}^d)$ to the positive definite cone $\mathbb{S}_+^{d-1}$.*

Proof. Let $\Gamma \in \mathcal{C}^d$. Since $\sigma_{\boldsymbol{b}}(\Gamma)$ is symmetric, it has real eigenvalues, and the eigenvectors are mutually orthogonal. It is clear that $\boldsymbol{b}^T \sigma_{\boldsymbol{b}}(\Gamma)\boldsymbol{b} = 0$, so $\boldsymbol{b}$ is an eigenvector with eigenvalue 0. We will show that all the other eigenvalues must be strictly positive. If $\boldsymbol{b} = \pm\frac{1}{d}\boldsymbol{1}$, then $\boldsymbol{x} \perp \boldsymbol{b}$, and $\boldsymbol{x} \neq \boldsymbol{0}$ implies that

$$\boldsymbol{x}^T \sigma(\Gamma)\boldsymbol{x} = \boldsymbol{x}^T\left(-\frac{1}{2}\Gamma\right)\boldsymbol{x} > 0$$

by the fact that Γ is strictly conditionally negative definite. This implies that all the remaining eigenvalues of $\sigma(\Gamma)$ must be strictly positive. Suppose now that $\boldsymbol{b} \neq \pm\frac{1}{d}\boldsymbol{1}$. By Proposition A.3, $\sigma_{\boldsymbol{b}}(\Gamma) = \boldsymbol{P}_{\boldsymbol{b}}\sigma(\Gamma)\boldsymbol{P}_{\boldsymbol{b}}^T$. Since $\boldsymbol{P}_{\boldsymbol{b}}^T\boldsymbol{x} = \boldsymbol{x} - (\boldsymbol{1}^T\boldsymbol{x})\boldsymbol{b}$, $\boldsymbol{P}_{\boldsymbol{b}}^T\boldsymbol{x} \perp \boldsymbol{1}$, and it follows that

$$(43) \qquad \boldsymbol{x}^T\sigma_{\boldsymbol{b}}(\Gamma)\boldsymbol{x} = \big(\boldsymbol{x} - \big(\boldsymbol{1}^T\boldsymbol{x}\big)\boldsymbol{b}\big)^T\sigma(\Gamma)\big(\boldsymbol{x} - \big(\boldsymbol{1}^T\boldsymbol{x}\big)\boldsymbol{b}\big) \geq 0$$

with strict inequality if $\boldsymbol{x} - (\mathbf{1}^T \boldsymbol{x})\boldsymbol{b} \neq \mathbf{0}$. However, $\boldsymbol{x} \perp \boldsymbol{b}$ and $\boldsymbol{b}^T \mathbf{1} = 1$ imply that $\boldsymbol{x}$ is not parallel to $\mathbf{1}$, and so we must have strict positivity in (43). $\qquad\square$

A.3. **Variograms in the positive case.** In our study of total positivity for extremes, we showed in Theorem 3.4 that a particularly important case is when $\Theta_{ij} \leq 0$ for all $i \neq j$. This is the case when Θ corresponds to a Laplacian matrix on a connected graph with positive weights on each edge. In this case $Q_{ij} = -\Theta_{ij} \geq 0$ for all $i \neq j$.

Recall from Remark A.6 and Lemma A.7 that if $\Gamma \in \mathcal{C}^d$, then Γ is always a distance matrix in the sense that $\sqrt{\Gamma_{ij}}$ are distances between a finite collection distinct points $\boldsymbol{y}_i$ for $i = 1, \ldots, d$ that lie in some Euclidean space $\mathbb{R}^p$. Let $U \in \mathbb{R}^{p \times d}$ be a matrix whose columns are $\boldsymbol{y}_1, \ldots, \boldsymbol{y}_d$. Note that translating all points $\boldsymbol{y}_i$ will not change mutual distances. We consider two important cases:

Case 1: We translate the points by their average so that now $\sum_i \boldsymbol{y}_i = \mathbf{0}$. In this case the Gram matrix $U^T U$ lies in $\mathbb{U}$, and in fact, it is equal to $\Sigma = \sigma(\Gamma)$.

Case 2: We translate the points to move one of the points to the origin so that now $\boldsymbol{y}_k = \mathbf{0}$ for some $k = 1, \ldots, d$. In this case $U^T U \in \mathbb{U}_k$, and in fact, it is equal to $\tilde{\Sigma}^{(k)} = \sigma_k(\Gamma)$.

In what follows, we outline some of interesting results of Miroslav Fiedler; see Fiedler (1998) and also an excellent overview in Devriendt (2022). Note that if $\Gamma \in \mathcal{C}^d$, then Σ and $\tilde{\Sigma}^{(k)}$ have rank $d - 1$. It implies that we can assume $k = d - 1$.

Lemma A.9. *If* $\Theta = \Sigma^+$ *is a Laplacian matrix of a weighted graph (with nonnegative weights), then* $\Sigma = U^T U$*, where* $U \in \mathbb{R}^{(d-1) \times d}$ *and the columns of* U *are vertices of a simplex, whose polar is hyperacute.*

For the proof, see Lemma 1 in Devriendt (2022).

As pointed out in Section D of Devriendt (2022), if Θ is a Laplacian matrix of a graph, then the entries of the corresponding matrix Γ are the effective resistances, and Γ is called the resistance matrix. The effective resistance allows the bijection between simplices, graphs and Laplacian matrices to be summarized beautifully by the following identity (see Theorem 2 in Devriendt (2022)).

Theorem A.10 (Fiedler's identity). *For a weighted graph with Laplacian* Θ *and resistance matrix* Γ*, the following identity holds:*

$$(44) \qquad -\frac{1}{2} \begin{bmatrix} 0 & \mathbf{1}^T \\ \mathbf{1} & \Gamma \end{bmatrix} = \begin{bmatrix} 4R^2 & -2\boldsymbol{r}^T \\ -2\boldsymbol{r} & \Theta \end{bmatrix}^{-1},$$

where $\boldsymbol{r} = \frac{1}{2}\Theta\xi + \frac{1}{d}\mathbf{1}$ *with* $\xi = \operatorname{diag}(\Sigma)$*, and* $R = \sqrt{\frac{1}{2}\xi^T(\boldsymbol{r} + \frac{1}{d}\mathbf{1})}$.

As we noted above, $\sqrt{\Gamma_{ij}}$ are always distances in the sense that the map $(i,j) \mapsto \sqrt{\Gamma_{ij}}$ is a metric function. However, if Θ is a Laplacian matrix, then the entries of Γ are effective resistances. By the next lemma we can conclude that, in this special case, the entries of Γ form a metric (see Klein and Randić (1993)).

Lemma A.11. *If* $\Theta_{ij} \leq 0$ *for all* $i \neq j$*, then the effective resistance* $(i,j) \mapsto \Gamma_{ij}$ *is a metric function.*

The implication in Proposition 3.6 cannot be reversed. There are situations when Γ is a metric, but Θ is not a Laplacian of a graph. In Proposition 3.6 we discussed exact conditions when it happens together with a probabilistic interpretation in terms of the association of the extremal function.

The fact that $(i,j) \mapsto \Gamma_{ij}$ is a metric does not give us a way to realize this metric as an Euclidean distance metric. The case we find particularly interesting is related with tree metrics (see, e.g., Semple et al. (2003)). Let T be an undirected tree with d leaves labeled with $[d]$. We say that $\Gamma \in \mathbb{S}_0^d$ forms

a tree metric over T if there exists edge length assignment $\theta_{uv} \geq 0$ for $uv \in T$ such that

$$\Gamma_{ij} = \sum_{uv \in \mathrm{ph}(i,j;T)} \theta_{uv}, \tag{45}$$

where $\mathrm{ph}(i,j;T)$ denotes the unique path between i and j in T.

Let T^k denote a rooted tree obtained from T by directing all edges away from a leaf $k \in [d]$. Note that

$$\widetilde{\Sigma}^{(k)}_{ij} = \frac{1}{2}(\Gamma_{ik} + \Gamma_{jk} - \Gamma_{ij}) = \sum_{uv \in \mathrm{ph}(i \wedge j, k;T)} \theta_{uv}, \tag{46}$$

where $i \wedge j$ denotes the most recent common ancestor of i and j in the tree T^k. But this means that the entries of $\Sigma^{(k)}$ lie in the Brownian motion tree model on the tree T^k; see Sturmfels et al. (2020) for more details. We get the following result.

Proposition A.12. *The image under σ_k of the set of all tree metrics over a given tree T is equal to the set of covariance matrices of the Brownian motion tree model over the rooted tree T^k.*

We finish by noting that the observation that the square root of a tree metric has an Euclidean embedding (which is a side product of this analysis) has been important for understanding some algorithms in phylogenetics Layer and Rhodes (2017).

Appendix B. Strong MTP$_2$ distributions

In this section we collect some new results on strongly MTP$_2$ distributions that will be later used in Appendix C to prove properties of EMTP$_2$ distributions. Results of this section may be of independent interest. The following lemma offers a useful characterization of strong MTP$_2$ distributions, as defined in (4).

Lemma B.1. *The function f is strongly MTP$_2$ if and only if for all $\mathbf{x}, \mathbf{y} \in \mathbb{R}^d$, and for all $s, t \geq c$ (for some $c \in \mathbb{R}$)*

$$f(\mathbf{x} - s\mathbf{1})f(\mathbf{y} - t\mathbf{1}) \leq f\big(\mathbf{x} \vee \mathbf{y} - (s \vee t)\mathbf{1}\big)f\big(\mathbf{x} \wedge \mathbf{y} - (s \wedge t)\mathbf{1}\big). \tag{47}$$

Proof. We first show that the strongly MTP$_2$ condition (4) implies the alternative (47). Suppose $t \geq s \geq c$. Let $\tilde{\mathbf{x}} = \mathbf{y} - t\mathbf{1}$, $\tilde{\mathbf{y}} = \mathbf{x} - s\mathbf{1}$ and $\alpha = t - s \geq 0$. We have $\tilde{\mathbf{x}} + \alpha\mathbf{1} = \mathbf{y} - s\mathbf{1}$ and $\tilde{\mathbf{y}} - \alpha\mathbf{1} = \mathbf{x} - t\mathbf{1}$. By (4)

$$f(\mathbf{x} - s\mathbf{1})f(\mathbf{y} - t\mathbf{1}) = f(\tilde{\mathbf{x}})f(\tilde{\mathbf{y}}) \leq f\big((\tilde{\mathbf{x}} + \alpha\mathbf{1}) \wedge \tilde{\mathbf{y}}\big)f\big(\tilde{\mathbf{x}} \vee (\tilde{\mathbf{y}} - \alpha\mathbf{1})\big)$$
$$= f(\mathbf{x} \wedge \mathbf{y} - s\mathbf{1})f(\mathbf{x} \vee \mathbf{y} - t\mathbf{1}),$$

which is exactly (47). If $c \leq t < s$, then we proceed in exactly the same way taking $\tilde{\mathbf{x}} = \mathbf{x} - s\mathbf{1}$, $\tilde{\mathbf{y}} = \mathbf{y} - t\mathbf{1}$ and $\alpha = s - t \geq 0$. This proves one implication. The other implication is obtained by reversing this argument. Fix $\mathbf{x}$, $\mathbf{y}$ and $\alpha \geq 0$. Suppose that (47) holds, and take $\tilde{\mathbf{x}} = \mathbf{x} + s\mathbf{1}$, $\tilde{\mathbf{y}} = \mathbf{y} + t\mathbf{1}$, $t = c$, $s = c + \alpha$. Then by (47),

$$f(\mathbf{x})f(\mathbf{y}) = f(\tilde{\mathbf{x}} - s\mathbf{1})f(\tilde{\mathbf{y}} - t\mathbf{1}) \leq f(\tilde{\mathbf{x}} \wedge \tilde{\mathbf{y}} - t\mathbf{1})f(\tilde{\mathbf{x}} \vee \tilde{\mathbf{y}} - s\mathbf{1})$$
$$= f\big((\mathbf{x} + \alpha\mathbf{1}) \wedge \mathbf{y}\big)f\big(\mathbf{x} \vee (\mathbf{y} - \alpha\mathbf{1})\big),$$

which is exactly (4). $\qquad\square$

We are now ready to prove Theorem 3.1.

Proof of Theorem 3.1. Observe that the density f of $\mathbf{Z}$ satisfies

$$(48) \qquad f(z_0, \mathbf{z}) = f_0(z_0) f_{\mathbf{X}}(\mathbf{z} - z_0 \mathbf{1}).$$

Proof of statement (1): Using (48), the MTP$_2$ constraint on f is equivalent to

$$(49) \qquad f_{\mathbf{X}}\big(\mathbf{x} \vee \mathbf{y} - (x_0 \vee y_0)\mathbf{1}\big) f_{\mathbf{X}}\big(\mathbf{x} \wedge \mathbf{y} - (x_0 \wedge y_0)\mathbf{1}\big) \geq f_{\mathbf{X}}(\mathbf{x} - x_0\mathbf{1}) f_{\mathbf{X}}(\mathbf{y} - y_0\mathbf{1})$$

for all $(x_0, \mathbf{x})$, $(y_0, \mathbf{y})$, where we used the fact that $f_0(x_0)f_0(y_0) = f_0(x_0 \vee y_0)f_0(x_0 \wedge y_0)$ (with both sides nonzero). But this condition is exactly equivalent to $f_{\mathbf{X}}$ being strongly MTP$_2$ by Lemma B.1.

Proof of statement (2): We first show the left implication via the equivalent characterization of strong MTP$_2$ from Lemma B.1. Denoting $\bar{\mathbf{x}} = (x_0, \mathbf{x})$ and $\bar{\mathbf{y}} = (y_0, \mathbf{y})$, we want to show that, for every $s \leq t$, it holds that

$$f(\bar{\mathbf{x}} - s\mathbf{1})f(\bar{\mathbf{y}} - t\mathbf{1}) \leq f(\bar{\mathbf{x}} \wedge \bar{\mathbf{y}} - s\mathbf{1})f(\bar{\mathbf{x}} \vee \bar{\mathbf{y}} - t\mathbf{1}),$$

where f as in (48). The left-hand side of this inequality is

$$L := f_0(x_0 - s)f_0(y_0 - t)f_X(\mathbf{x} - x_0\mathbf{1})f_X(\mathbf{y} - y_0\mathbf{1}),$$

and the right-hand side is

$$R := f_0(x_0 \wedge y_0 - s)f_0(x_0 \vee y_0 - t)f_X\big(\mathbf{x} \wedge \mathbf{y} - (x_0 \wedge y_0)\mathbf{1}\big)f_X\big(\mathbf{x} \vee \mathbf{y} - (x_0 \vee y_0)\mathbf{1}\big).$$

In the proof of statement (1), we established that the strongly MTP$_2$ property of $\mathbf{X}$ gives that $\mathbf{Z}$ is MTP$_2$. In other words, the inequality (49) holds. Given this inequality, to show $L \leq R$ it is certainly enough to show that

$$f_0(x_0 - s)f_0(y_0 - t) \leq f_0(x_0 \wedge y_0 - s)f_0(x_0 \vee y_0 - t),$$

which holds if f_0 is strongly MTP$_2$ by Lemma B.1. For the other direction, note that by statement (1), we have that $\mathbf{X}$ is strongly MTP$_2$ as $\mathbf{Z}$ is MTP$_2$. To conclude that X_0 is strongly MTP$_2$, we will show that strongly MTP$_2$ distributions are closed under marginalization. This will conclude the proof of the second statement, as X_0 is a component of $\mathbf{Z}$.

Strongly MTP$_2$ distributions are closed under taking margins: Suppose that the random vector $\mathbf{X} = (X_1, \ldots, X_d)$ is strongly MTP$_2$. We will show that $(X_1, \ldots, X_{d-1})$ is strongly MTP$_2$. By statement (1) $\mathbf{X}$ is strongly MTP$_2$ if and only if for every X_0 independent of $\mathbf{X}$ and supported on $[c, \infty)$ for some fixed $c \in \mathbb{R}$, the vector $(X_0, X_0 + X_1, \ldots, X_0 + X_d)$ is MTP$_2$. By the closure property of the MTP$_2$ distributions, the vector $(X_0, X_0 + X_1, \ldots, X_0 + X_{d-1})$ is also MTP$_2$ for every such X_0. Again, using statement (1), this is equivalent to $(X_1, \ldots, X_{d-1})$ being strongly MTP$_2$. The same argument applies to any other margin. $\qquad\square$

In the proof of Theorem 3.1, we showed that also strong MTP$_2$ is closed under taking margins.

Proposition B.2. *If $\mathbf{X}$ is strongly* MTP$_2$*, then every margin of $\mathbf{X}$ is strongly* MTP$_2$*.*

Example 10. It is useful to see Theorem 3.1 in action in the context of Gaussian distributions. If Σ is the covariance matrix of $\mathbf{X}$ and v is the variance of X_0, then the covariance of $\mathbf{Z}$ has the block form

$$\begin{bmatrix} v & v\mathbf{1}^T \\ v\mathbf{1} & \Sigma + v\mathbf{1}\mathbf{1}^T \end{bmatrix}$$

with the inverse

$$\begin{bmatrix} v^{-1} + \mathbf{1}^T\Sigma^{-1}\mathbf{1} & -\mathbf{1}^T\Sigma^{-1} \\ -\Sigma^{-1}\mathbf{1} & \Sigma^{-1} \end{bmatrix}.$$

It is then clear that this is an M-matrix (equiv. $\mathbf{Y}$ is MTP$_2$) if and only if Σ^{-1} is an M-matrix with $\mathbf{1}^T\Sigma^{-1} \geq 0$ (equiv. $\mathbf{X}$ is strongly MTP$_2$), which is precisely part 1 of the theorem. For the second

part, we note that the last matrix above has row sums $(v^{-1}, 0, \ldots, 0)$. If $\mathbf{X}$ is strongly MTP$_2$, then it also forms an M-matrix, and so $\mathbf{Z}$ is strongly MTP$_2$.

Another important property that we mentioned in Section 2.1 is that univariate distributions are always MTP$_2$. This result is not true for strong MTP$_2$. A random vector $\mathbf{X}$ is log-concave if its density is log-concave.

Proposition B.3. *A univariate distribution with density $f : \mathbb{R} \to \mathbb{R}$ is strongly MTP$_2$ if and only if it is log-concave. A random vector $\mathbf{X} = (X_1, \ldots, X_d)$ with independent components is strongly MTP$_2$ if and only if each X_i is log-concave.*

Proof. Note that (4) with $d = 1$ becomes nontrivial, only if $0 \le \alpha \le y - x$ in which case if gives $f(y - \alpha)f(x + \alpha) - f(x)f(y) \ge 0$. Let $F : \mathbb{R} \to \mathbb{R} \cup \{-\infty\}$ be defined by $F(x) = -\log f(x)$. Denoting $\alpha = \lambda(y - x)$ for $\lambda \in [0, 1]$, we get

$$\big(F\big((1 - \lambda)x + \lambda y\big) - (1 - \lambda)F(x) - \lambda F(y)\big)$$
$$+ \big(F\big(\lambda x + (1 - \lambda)y\big) - \lambda F(x) - (1 - \lambda)F(y)\big) \le 0.$$

Taking $\lambda = \frac{1}{2}$, we conclude midpoint convexity of F, which is equivalent to concavity as $x < y$ are arbitrary. On the other hand, convexity of F trivially implies the above inequality, which is equivalent to the strongly MTP$_2$ inequality.

For the second statement, let $F(\mathbf{x}) = -\log f_X(\mathbf{x})$ so that $F(\mathbf{x}) = \sum_i F_i(x_i)$, where $F_i = -\log f_i$. We want to show that for each $\mathbf{x}, \mathbf{y} \in \mathbb{R}^d$, $\alpha \ge 0$

$$\sum_i \big(F_i(x_i) + F_i(y_i) - F_i\big(x_i \vee (y_i - \alpha)\big) - F_i\big((x_i + \alpha) \wedge y_i\big)\big) \ge 0$$

if and only if each summand is nonnegative. The left implication is obvious. But the right implication is also clear using the insights of the proof of the univariate case. Simply take $\mathbf{x}, \mathbf{y}$ such that $x_i > y_i$ for all $i \ne k$. The corresponding summands are zero and so necessarily $F_k(x_k) + F_k(y_k) - F_k(x_k \vee (y_k - \alpha)) - F_i((x_k + \alpha) \wedge y_k) \ge 0$. $\qquad\square$

B.1. **Log-concave tree processes.** Theorem 3.1 and Proposition B.3 give a natural way to construct multivariate strongly MTP$_2$ distributions with log-concave distributions. If $X_1, \ldots, X_d$ are univariate log-concave and independent, then

$$(50) \qquad\qquad (X_1, X_1 + X_2, X_1 + X_2 + X_3, \ldots, X_1 + \cdots + X_d)$$

is strongly MTP$_2$ and log-concave. We now provide a generalization of this construction.

Let $T = (V, E)$ be an undirected tree with vertex set $V = \{1, \ldots, d\}$. A rooted tree T^k is a tree obtained from T by choosing a vertex $k \in V$, called the root, and directing all edges away from k. For any two nodes i, j in an undirected tree T, we denote by $\mathrm{ph}(ij; T)$ the set of edges on the (unique) path between i and j in this tree. Equivalently, for a rooted tree T^k, let $\mathrm{ph}(ij; T^k)$ be the set of directed edges on the (unique) path from i to j in T^k.

Definition 3. For a given rooted tree T^k with vertices $V = \{1, \ldots, d\}$, let $X_1, \ldots, X_d$ be a collection of independent random variables. Let $\mathbf{Z} = (Z_1, \ldots, Z_d)$ be defined by

$$(51) \qquad\qquad Z_i = X_k + \sum_{uv \in \mathrm{ph}(ki; T^k)} X_v,$$

where uv denotes a directed edge $u \to v$. Then we say that $\mathbf{Z}$ follows an additive process on T^k. If all X_i are log-concave, then we call such process a log-concave process on a tree.

For example, if $d = 3$, the vector in (50) forms an additive process on the tree $1 \to 2 \to 3$. Rerooting this tree at 2 results in an additive process $(X_1 + X_2, X_2, X_2 + X_3)$.

Proposition B.4. *If* $\mathbf{Z}$ *follows a log-concave tree process, then it has a strongly* MTP_2 *and log-concave distribution.*

Proof. Since X_k is log-concave, then by Theorem 3.1 the vector $\mathbf{Z}$ is strongly MTP_2 as long as $(Z_i - Z_k)_{i \neq k}$ is strongly MTP_2. This vector can be split into independent components indexed by the children of k in T^k. In each of the components, we apply the same argument recursively. The fact that concatenating independent strongly MTP_2 vectors gives a strongly MTP_2 vector is clear. $\qquad\square$

A special case of the construction in Proposition B.4 is when $\mathbf{X}$ is independent zero-mean Gaussian. In this case the set of marginal distributions over the leaves of T is called the Brownian motion tree model (Felsenstein (1973)); see, for example, Section 2 in Sturmfels et al. (2020) for the structural equation representation, as in (51). Since the distribution of $\mathbf{Z}$ is strongly MTP_2, this property is preserved in the margin by Proposition B.2. We recover a well-known fact that the inverse covariance matrix in a Brownian motion tree model is always a diagonally dominant M-matrix; see, for example, Dellacherie et al. (2014), where the covariance matrices in the Brownian motion tree model are called simply tree matrices. In extreme value theory, we encounter such construction in the context of the extremal tree models (see Section 4.1).

Appendix C. Auxiliary results and proofs

C.1. **The exponent measure** Λ. We use here the notation of Section 2.2.

In order to describe the extremal dependence structure, the assumption of multivariate regular variation is widely used (Resnick (2008)). Formally, it is equivalent to the existence of the limit

$$(52) \qquad \lim_{u \to \infty} u\big[1 - \mathbb{P}(\mathbf{X} \leq \mathbf{z} + u\mathbf{1})\big] = \Lambda(\mathbf{z})$$

for all $\mathbf{z} \in \mathcal{E} = [-\infty, \infty)^d \setminus \{(-\infty, \ldots, -\infty)\}$. The exponent measure Λ is a Radon measure on $\mathcal{E}$, and $\Lambda(\mathbf{z})$ is the short-hand notation for $\Lambda(\mathcal{E} \setminus [(-\infty, \ldots, -\infty), \mathbf{z}])$. The fact that Λ arises as a limit in (52) implies a homogeneity property $\Lambda(\mathbf{z} + t\mathbf{1}) = t^{-1}\Lambda(\mathbf{z})$, for any $t > 0$. If we assume that Λ possesses a positive Lebesgue density λ, then it satisfies $\lambda(\mathbf{y} + t\mathbf{1}) = t^{-1}\lambda(\mathbf{y})$ for any $t > 0$ and $\mathbf{y} \in \mathbb{R}^d$. The Ith marginal λ_I of λ is defined for any nonempty $I \subset [d] := \{1, \ldots, d\}$, as usual by integrating out all components in $[d] \setminus I$.

The relation of the exponent measure to the multivariate Pareto distribution $\mathbf{Y}$ is the following:

$$(53) \qquad \mathbb{P}(\mathbf{Y} \leq \mathbf{z}) = \frac{\Lambda(\mathbf{z} \wedge \mathbf{0}) - \Lambda(\mathbf{z})}{\Lambda(\mathbf{0})}, \quad \mathbf{z} \in \mathcal{L}.$$

From this it follows that the density $f_{\mathbf{Y}}$ of $\mathbf{Y}$ satisfies $f_{\mathbf{Y}}(\mathbf{y}) = \lambda(\mathbf{y})/\Lambda(\mathbf{0})$. Similarly, the random vector $\mathbf{Y}^k$ has Lebesgue density λ supported on the product space $\mathcal{L}^k$.

C.2. **Proof of Theorem 3.2.** We first prove the last statement that the condition holds for one k if and only if it holds for all k. Note that $\mathbf{Y}^k$ has density $\lambda(\mathbf{y})$ and is supported on the product space $\mathcal{L}^k$. Assume that $\mathbf{Y}^k$ is MTP_2, that is, that $\lambda(\mathbf{y})$ satisfies (3) on $\mathcal{L}^k$. For any $k' \in [d]$, there exists some $t > 0$ such that, for any $\mathbf{x}, \mathbf{y} \in \mathcal{L}^{k'}$, it holds that $\mathbf{x} + t\mathbf{1}, \mathbf{y} + t\mathbf{1}, (\mathbf{x} \wedge \mathbf{y}) + t\mathbf{1}, (\mathbf{x} \vee \mathbf{y}) + t\mathbf{1} \in \mathcal{L}^k$. Hence, it follows from the homogeneity of λ that

$$\begin{aligned}
\lambda(\mathbf{x} \vee \mathbf{y})\lambda(\mathbf{x} \wedge \mathbf{y}) &= t^2 \lambda\big((\mathbf{x} \vee \mathbf{y}) + t\mathbf{1}\big)\lambda\big((\mathbf{x} \wedge \mathbf{y}) + t\mathbf{1}\big) \\
&\geq t^2 \lambda(\mathbf{x} + t\mathbf{1})\lambda(\mathbf{y} + t\mathbf{1}) \\
&= \lambda(\mathbf{x})\lambda(\mathbf{y}).
\end{aligned}$$

Now, to prove the first statement, we see that it is enough to check this condition on one k, so without loss of generality take $k = d$. Using (7) we have $Y_d^d = E$ and $Y_i^d = E + W_i^d$ for $i = 1, \ldots, d-1$.

Since E is exponentially distributed, we can use Theorem 3.1 to conclude that $\mathbf{Y}^d$ is MTP$_2$ if and only if the vector $\mathbf{W}_{\backslash d}^d$ is strongly MTP$_2$.

C.3. **Proof of Proposition 3.3.** Let $\mathbf{Y}$ be EMTP$_2$. This means that for all $k \in V$, the vector $\mathbf{Y}^k$ is MTP$_2$. Let $\mathbf{Y}_I$ be the marginal of $\mathbf{Y}$ for some $I \subset V$. It holds that

$$\mathbf{Y}_I | Y_k > 0 \overset{d}{=} \left(\mathbf{Y}^k\right)_I \quad \text{for all } k \in I;$$

see Engelke and Hitz (2020). As MTP$_2$ is closed under taking margins, the proposition follows.

C.4. **Proof of Theorem 3.4.** By Theorem 3.2, $\mathbf{Y}$ is EMTP$_2$ if and only if each $\mathbf{W}^k$ is strongly MTP$_2$. By Example 1, equivalently, each $\Theta^{(k)}$ is a diagonally dominant M-matrix. This establishes that $\mathbf{Y}$ being EMTP$_2$ is equivalent to (ii).

On the other hand, Θ being a Laplacian of a connected graph with positive edge weights is equivalent with the seemingly simpler condition (i). The fact that $\Theta \in \mathbb{U}_+^d$ implies (i) is clear. For the other direction, note that, by Proposition 2.2, the row sums of Θ are zero and $\Theta_{ij} \leq 0$ for all $i \neq j$. It follows that Θ is a Laplacian matrix of a graph weighted with $Q_{ij} = -\Theta_{ij} \geq 0$. Since Γ is strictly conditionally negative definite, again by Proposition 2.2, $\text{rank}(\Theta) = d - 1$. It then follows thaat $\det(\Theta^{(k)}) > 0$. By (23) we conclude that at least one of the tree terms is strictly positive, proving that the underlying graph is connected, that is, $\Theta \in \mathbb{U}_+^d$.

The proof will be then concluded if we establish equivalence between conditions (i)–(iv). Note first that all these conditions hold simultaneously for all bivariate Hüsler–Reiss distributions; compare Example 4. Thus, we assume $d \geq 3$. In all cases we heavily rely on Lemma A.4. In particular, if (i) holds, then the formula $\Theta_{ij}^{(k)} = \Theta_{ij}$ for $i, j \neq k$ implies that $\Theta^{(k)}$ is an M-matrix and the formula $\sum_{l \neq k} \Theta_{il}^{(k)} = -\Theta_{ik}$ implies that each $\Theta^{(k)}$ is also diagonally dominant. In other words, (i) implies all (ii), (iii) and (iv).

Since (iv) is weaker than (ii), it remains to show that both (iii) and (iv) imply (i).

(iii) $\Rightarrow$ (i): To show that $\Theta_{ij} \leq 0$, we take any $k \neq i, j$ (there will be at least one as $d \geq 3$) and use again the formula $\Theta_{ij} = \Theta_{ij}^{(k)} \leq 0$.

(iv) $\Rightarrow$ (i): Suppose $\Theta^{(k)}$ is a diagonally dominant M-matrix. By the same argument as above, this is enough to conclude $\Theta_{ij} \leq 0$ for all $i, j \neq k$. Similarly, as above, $\Theta_{ik} = -\sum_{l \neq k} \Theta_{il}^{(k)} \leq 0$ because $\Theta^{(k)}$ is diagonally dominant.

C.5. **Proof of Proposition 3.6.** For a Hüsler–Reiss random vector $\mathbf{Y}$, it holds that $\mathbf{W}^k$ is associated if and only if $\Sigma^{(k)}$ is nonnegative. Since $\mathbf{W}_{\backslash k}^k$ is Gaussian with covariance matrix $\Sigma^{(k)}$, this is equivalent with $\Sigma^{(k)} \geq 0$ by Pitt (1982). Now, the result follows from the fact that

$$\Sigma_{ij}^{(k)} \geq 0 \quad \Longleftrightarrow \quad \Sigma_{ii}^{(k)} + \Sigma_{jj}^{(k)} \geq \Sigma_{ii}^{(k)} + \Sigma_{jj}^{(k)} - 2\Sigma_{ij}^{(k)} \quad \Longleftrightarrow \quad \Gamma_{ik} + \Gamma_{jk} \geq \Gamma_{ij}$$

for all $i, j, k \in [d]$.

C.6. **Proof of Proposition 3.7.** By Theorem 3.2, $\mathbf{Y}$ is EMTP$_2$ if and only if $\mathbf{W}_{\backslash d}^d = (U_i - U_d)_{i \neq d}$ is strongly MTP$_2$. Let $X_0 = -U_d$ and $X_i = U_i$ for $i = 1, \ldots, d-1$. Denoting $\mathbf{X} = (X_1, \ldots, X_{d-1})$, the fact that $\mathbf{X}$ is strongly MTP$_2$ follows from Proposition B.3, as the distribution of each X_i is log-concave. By assumption the distribution of $-X_0$ is also log-concave, and so the distribution of X_0 must be log-concave. It follows from Theorem 3.1 that the vector $(X_0, X_0 + X_1, \ldots, X_0 + X_{d-1})$ is strongly MTP$_2$. Since the strong MTP$_2$ property is closed under taking margins (Proposition B.2), we conclude that

$$(X_0 + X_1, \ldots, X_0 + X_{d-1}) = (U_1 - U_d, \ldots, U_{d-1} - U_d)$$

is strongly MTP$_2$, proving that $\mathbf{Y}$ is EMTP$_2$.

C.7. **Proof of Theorem 3.8.** By Theorem 3.2, EMTP$_2$ is equivalent to W_2^1 being strongly MTP$_2$. But this is a univariate random variable, so equivalently, its density must be log-concave by Proposition B.3.

C.8. **Proof of Proposition 4.1.** By Theorem 3.2, we need to check whether $\mathbf{W}_{\setminus k}^k$ is strongly MTP$_2$. By (17) it follows that

$$Y_i^k = E + \sum_{e \in \mathrm{ph}(ki; T^k)} W_e,$$

where $W_e, e \in T^k$ are independent. As E is log-concave, by Proposition B.4 we have that $\mathbf{Y}^k$ is strongly MTP$_2$ if and only if W_e is log-concave for each $e \in E$. This is equivalent to $\mathbf{W}_{\setminus k}^k$ being strongly MTP$_2$ by Theorem 3.1(2). From Example 4 it then follows that Hüsler–Reiss tree models are always EMTP$_2$.

C.9. **Proof of Theorem 4.4.** Since by definition $\mathbf{Y} \sim \mathbb{P}_{\mathbf{Y}}$ satisfies the pairwise Markov property with respect to its pairwise independence graph $G_e(\mathbb{P}_{\mathbf{Y}})$ and since it has a positive and continuous density, it also satisfies the global Markov property. Indeed, since the density of $\mathbf{Y}^k$ is proportional to the density of $\mathbf{Y}$, it is also positive and continuous. Lauritzen (1996, Chapter 3) shows the equivalence of the pairwise and the global Markov property in this case for $\mathbf{Y}^k$, and this then propagates to the corresponding extremal conditional independence properties by Definition 1. Therefore, $\mathbf{Y}$ satisfies the global Markov property with respect to $G_e(\mathbb{P}_{\mathbf{Y}})$.

Assume disjoint $A, B, C \subset V$ such that C does not separate A from B in $G_e(\mathbb{P}_{\mathbf{Y}})$. We need to show that that $\mathbf{Y}_A \not\perp_e \mathbf{Y}_B | \mathbf{Y}_C$ to conclude that $\mathbb{P}_{\mathbf{Y}}$ is extremal faithful to $G_e(\mathbb{P}_{\mathbf{Y}})$. To see this, let $(k, l) \in E(G_e(\mathbb{P}_{\mathbf{Y}}))$ with $k, l \notin C$, which means that $Y_k \not\perp_e Y_l | \mathbf{Y}_{V \setminus kl}$. As $\mathbf{Y}$ is EMTP$_2$, upward-stability (see Theorem 4.2) implies that $Y_k \not\perp_e Y_l | \mathbf{Y}_C$. As C does not separate A from B, there is a path in $G_e(\mathbb{P}_{\mathbf{Y}})$ from some $i \in A$ to some $j \in B$ that does not intersect C. It holds that $Y_s \not\perp_e Y_t | \mathbf{Y}_C$ for any edge (s, t) on the path from i to j. As $\mathbf{Y}$ is EMTP$_2$, it satisfies singleton-transitivity (see Theorem 4.2) such that for edges (s, t), (t, u) on the path from i to j it follows that $Y_s \not\perp_e Y_u | \mathbf{Y}_C \vee Y_s \not\perp_e Y_u | \mathbf{Y}_{tC}$. Now, using again upward stability, we obtain that $Y_s \not\perp_e Y_u | \mathbf{Y}_{tC}$ implies $Y_s \not\perp_e Y_u | \mathbf{Y}_C$. This gives that $Y_i \not\perp_e Y_j | \mathbf{Y}_C$. With Remark 4.3 the theorem follows.

C.10. **Proof of Lemma 5.1.** We use the notation of Appendix A, where $\tilde{S}^{(k)}$ is the embedding of $S^{(k)} \in \mathbb{S}^{d-1}$ in $\mathbb{S}^d$ by adding to it a zero row/column (as the kth row/column). Similarly, $\tilde{\Theta}^{(k)}$ is the pseudoinverse of $\tilde{\Sigma}^{(k)}$. Note that $\langle S^{(k)}, \Theta^{(k)} \rangle = \langle \tilde{S}^{(k)}, \tilde{\Theta}^{(k)} \rangle$, which is equal to $\langle\!\langle \overline{\Gamma}, Q \rangle\!\rangle$ simply because both are equal to $\langle\!\langle \overline{\Gamma}, Q \rangle\!\rangle$ by Remark A.1(4). This gives

$$\langle S^{(k)}, \Theta^{(k)} \rangle = \langle S, \Theta \rangle = \langle\!\langle \overline{\Gamma}, Q \rangle\!\rangle.$$

Moreover, by (23)

$$\log \det \Theta^{(k)} = \log\left(\sum_{T \in \mathcal{T}} \prod_{ij \in T} Q_{ij} \right) = \log \mathrm{Det}\, \Theta - \log(d).$$

This proves both (24) and (25).

References

Agrawal, R., U. Roy, and C. Uhler (2020). Covariance matrix estimation under total positivity for portfolio selection. *Journal of Financial Econometrics*.

Asadi, P., A. C. Davison, and S. Engelke (2015). Extremes on river networks. *Ann. Appl. Stat. 9*(4), 2023–2050.

Asenova, S., G. Mazo, and J. Segers (2021). Inference on extremal dependence in the domain of attraction of a structured Hüsler-Reiss distribution motivated by a Markov tree with latent variables. *Extremes 24*(3), 461–500.

Banerjee, O., L. El Ghaoui, and A. d'Aspremont (2008). Model selection through sparse maximum likelihood estimation for multivariate Gaussian or binary data. *J. Mach. Learn. Res. 9*, 485–516.

Berge, C. (1997). *Topological spaces.* Dover Publications, Inc., Mineola, NY. Including a treatment of multi-valued functions, vector spaces and convexity, Translated from the French original by E. M. Patterson, Reprint of the 1963 translation.

Coles, S., J. Heffernan, and J. Tawn (1999). Dependence measures for extreme value analyses. *Extremes 2*(4), 339–365.

Coles, S. G. and J. A. Tawn (1991). Modelling extreme multivariate events. *J. Roy. Statist. Soc. Ser. B 53*(2), 377–392.

Cooley, D., P. Naveau, and P. Poncet (2006). Variograms for spatial max-stable random fields. In P. Bertail, P. Soulier, and P. Doukhan (Eds.), *Dependence in Probability and Statistics*, Volume 187 of *Lecture Notes in Statistics*, Chapter 17, pp. 373–390. New York: Springer.

Cooley, D. and E. Thibaud (2019). Decompositions of dependence for high-dimensional extremes. *Biometrika 106*(3), 587–604.

de Haan, L. and A. Ferreira (2006). *Extreme Value Theory.* New York: Springer.

de Haan, L. and S. I. Resnick (1977). Limit theory for multivariate sample extremes. *Z. Wahrscheinlichkeitstheorie und Verw. Gebiete 40*(4), 317–337.

Dellacherie, C., S. Martinez, and J. San Martin (2014). *Inverse M-matrices and ultrametric matrices*, Volume 2118. Springer.

Devriendt, K. (2022). Effective resistance is more than distance: Laplacians, simplices and the Schur complement. *Linear Algebra Appl. 639*, 24–49.

Deza, M. M. and M. Laurent (1997). *Geometry of cuts and metrics*, Volume 15 of *Algorithms and Combinatorics.* Springer-Verlag, Berlin.

Dombry, C., S. Engelke, and M. Oesting (2016). Exact simulation of max-stable processes. *Biometrika 103*(2), 303–317.

Dombry, C. and F. Eyi-Minko (2013). Regular conditional distributions of continuous max-infinitely divisible random fields. *Electron. J. Probab. 18*, no. 7, 21.

Drees, H. and A. Sabourin (2021). Principal component analysis for multivariate extremes. *Electron. J. Stat. 15*(1), 908–943.

Duval, A. M., C. J. Klivans, and J. L. Martin (2009). Simplicial matrix-tree theorems. *Trans. Amer. Math. Soc. 361*(11), 6073–6114.

Egilmez, H. E., E. Pavez, and A. Ortega (2017). Graph learning from data under Laplacian and structural constraints. *IEEE Journal of Selected Topics in Signal Processing 11*(6), 825–841.

Einmahl, J. H. J., A. Kiriliouk, A. Krajina, and J. Segers (2016). An *M*-estimator of spatial tail dependence. *Journal of the Royal Statistical Society. Series B. Statistical Methodology 78*(1), 275–298.

Einmahl, J. H. J. and J. Segers (2009). Maximum empirical likelihood estimation of the spectral measure of an extreme-value distribution. *The Annals of Statistics 37*, 2953–2989.

Embrechts, P., C. Klüppelberg, and T. Mikosch (1997). *Modelling Extremal Events: for Insurance and Finance*. London: Springer.

Engelke, S. and A. S. Hitz (2020). Graphical models for extremes. *J. R. Stat. Soc. Ser. B. Stat. Methodol. 82*(4), 871–932. With discussions.

Engelke, S., A. S. Hitz, N. Gnecco, and M. Hentschel (2022). *graphicalExtremes: Statistical Methodology for Graphical Extreme Value Models*. R package version 0.2.0.

Engelke, S. and J. Ivanovs (2021). Sparse structures for multivariate extremes. *Annu. Rev. Stat. Appl. 8*, 241–270.

Engelke, S., A. Malinowski, Z. Kabluchko, and M. Schlather (2015). Estimation of Hüsler-Reiss distributions and Brown-Resnick processes. *J. R. Stat. Soc. Ser. B. Stat. Methodol. 77*(1), 239–265.

Engelke, S., T. Opitz, and J. Wadsworth (2019). Extremal dependence of random scale constructions. *Extremes 22*(4), 623–666.

Engelke, S. and S. Volgushev (2022). Structure learning for extremal tree models. *J. R. Stat. Soc. Ser. B. Stat. Methodol. 84*(5), 2055–2087.

Esary, J. D., F. Proschan, and D. W. Walkup (1967). Association of random variables, with applications. *Ann. Math. Statist. 38*, 1466–1474.

Fallat, S., S. Lauritzen, K. Sadeghi, C. Uhler, N. Wermuth, and P. Zwiernik (2017). Total positivity in Markov structures. *The Annals of Statistics 45*(3), 1152–1184.

Felsenstein, J. (1973). Maximum-likelihood estimation of evolutionary trees from continuous characters. *American journal of human genetics 25*(5), 471.

Fiedler, M. (1998). Some characterizations of symmetric inverse M-matrices. In *Proceedings of the Sixth Conference of the International Linear Algebra Society (Chemnitz, 1996)*, Volume 275/276, pp. 179–187.

Fomichov, V. and J. Ivanovs (2023). Spherical clustering in detection of groups of concomitant extremes. *Biometrika 110*(1), 135–153.

Fortuin, C. M., P. W. Kasteleyn, and J. Ginibre (1971). Correlation inequalities on some partially ordered sets. *Communications in Mathematical Physics 22*, 89–103.

Gnecco, N., N. Meinshausen, J. Peters, and S. Engelke (2021). Causal discovery in heavy-tailed models. *Ann. Statist. 49*(3), 1755–1778.

Gower, J. C. (1985). Properties of Euclidean and non-Euclidean distance matrices. *Linear Algebra and its Applications 67*, 81–97.

Hashorva, E. (2012). Exact tail asymptotics in bivariate scale mixture models. *Extremes 15*(1), 109–128.

Heffernan, J. E. and J. A. Tawn (2004). A conditional approach for multivariate extreme values. *J. R. Stat. Soc. Ser. B Stat. Methodol. 66*(3), 497–546. With discussions and reply by the authors.

Hentschel, M., S. Engelke, and J. Segers (2022). Statistical inference for Hüsler–Reiss graphical models through matrix completions. *arXiv preprint arXiv:2210.14292*.

Holbrook, A. (2018). Differentiating the pseudo determinant. *Linear Algebra Appl. 548*, 293–304.

Holland, P. W. and P. R. Rosenbaum (1986). Conditional association and unidimensionality in monotone latent variable models. *Ann. Statist. 14*(4), 1523–1543.

Horn, R. A. and C. R. Johnson (2013). *Matrix analysis* (Second ed.). Cambridge University Press, Cambridge.

Hüsler, J. and R.-D. Reiss (1989). Maxima of normal random vectors: between independence and complete dependence. *Statist. Probab. Lett. 7*(4), 283–286.

Karlin, S. and Y. Rinott (1980). Classes of orderings of measures and related correlation inequalities. I. Multivariate totally positive distributions. *Journal of Multivariate Analysis 10*(4), 467–498.

Klein, D. J. and M. Randić (1993). Resistance distance. *J. Math. Chem. 12*(1-4), 81–95. Applied graph theory and discrete mathematics in chemistry (Saskatoon, SK, 1991).

Krijnen, W. P. (2004). Positive loadings and factor correlations from positive covariance matrices. *Psychometrika 69*(4), 655–660.

Krupskii, P., R. Huser, and M. G. Genton (2018). Factor copula models for replicated spatial data. *J. Amer. Statist. Assoc. 113*(521), 467–479.

Larsson, M. and S. I. Resnick (2012). Extremal dependence measure and extremogram: the regularly varying case. *Extremes 15*(2), 231–256.

Lauritzen, S. and K. Sadeghi (2018). Unifying Markov properties for graphical models. *Ann. Statist. 46*(5), 2251–2278.

Lauritzen, S., C. Uhler, and P. Zwiernik (2019). Maximum likelihood estimation in Gaussian models under total positivity. *Ann. Statist. 47*(4), 1835–1863.

Lauritzen, S., C. Uhler, and P. Zwiernik (2021). Total positivity in exponential families with application to binary variables. *Ann. Statist. 49*(3), 1436–1459.

Lauritzen, S. and P. Zwiernik (2020). *GOLAZO: Flexible regularised likelihood estimation using the GOLAZO approach.* Available from https://github.com/pzwiernik/golazo.

Lauritzen, S. and P. Zwiernik (2022). Locally associated graphical models and mixed convex exponential families. *Ann. Statist. 50*(5), 3009–3038.

Lauritzen, S. L. (1996). *Graphical models*, Volume 17 of *Oxford Statistical Science Series*. The Clarendon Press, Oxford University Press, New York. Oxford Science Publications.

Lawley, D. N. and A. E. Maxwell (1962). Factor analysis as a statistical method. *Journal of the Royal Statistical Society. Series D (The Statistician) 12*(3), 209–229.

Layer, M. and J. A. Rhodes (2017). Phylogenetic trees and Euclidean embeddings. *J. Math. Biol. 74*(1-2), 99–111.

Liu, Y. and T. J. Kozubowski (2015). A folded Laplace distribution. *Journal of Statistical Distributions and Applications 2*(1), 1–17.

Marshall, A. W. and I. Olkin (1983). Domains of attraction of multivariate extreme value distributions. *Ann. Probab. 11*(1), 168–177.

Mhalla, L., V. Chavez-Demoulin, and D. J. Dupuis (2020). Causal mechanism of extreme river discharges in the upper Danube basin network. *J. R. Stat. Soc. Ser. C. Appl. Stat. 69*(4), 741–764.

Micchelli, C. A. (1986). Interpolation of scattered data: distance matrices and conditionally positive definite functions. *Constr. Approx. 2*(1), 11–22.

Murota, K. (2009). Recent developments in discrete convex analysis. In *Research trends in combinatorial optimization*, pp. 219–260. Springer.

Newman, C. M. (1983). A general central limit theorem for FKG systems. *Comm. Math. Phys. 91*(1), 75–80.

Newman, C. M. (1984). Asymptotic independence and limit theorems for positively and negatively dependent random variables. *5*, 127–140.

Papastathopoulos, I. and K. Strokorb (2016). Conditional independence among max-stable laws. *Statist. Probab. Lett. 108*, 9–15.

Pearl, J. (2009). *Causality* (Second ed.). Cambridge University Press, Cambridge. Models, reasoning, and inference.

Pitt, L. D. (1982). Positively correlated normal variables are associated. *Ann. Probab. 10*(2), 496–499.

Ravikumar, P., M. J. Wainwright, G. Raskutti, and B. Yu (2011). High-dimensional covariance estimation by minimizing ℓ_1-penalized log-determinant divergence. *Electron. J. Stat. 5*, 935–980.

Resnick, S. I. (2008). *Extreme Values, Regular Variation and Point Processes.* New York: Springer.

Robeva, E., B. Sturmfels, N. Tran, and C. Uhler (2021). Maximum likelihood estimation for totally positive log-concave densities. *Scand. J. Stat. 48*(3), 817–844.

Rootzén, H. and N. Tajvidi (2006). Multivariate generalized Pareto distributions. *Bernoulli 12*(5), 917–930.

Rossell, D. and P. Zwiernik (2021). Dependence in elliptical partial correlation graphs. *Electron. J. Stat. 15*(2), 4236–4263.

Schlather, M. and J. A. Tawn (2003). A dependence measure for multivariate and spatial extreme values: properties and inference. *Biometrika 90*(1), 139–156.

Schoenberg, I. J. (1935). Remarks to Maurice Fréchet's article "Sur la définition axiomatique d'une classe d'espace distanciés vectoriellement applicable sur l'espace de Hilbert" [MR1503246]. *Annals of Mathematics. Second Series 36*(3), 724–732.

Segers, J. (2020). One- versus multi-component regular variation and extremes of Markov trees. *Adv. in Appl. Probab. 52*(3), 855–878.

Semple, C., M. Steel, et al. (2003). *Phylogenetics*, Volume 24. Oxford University Press on Demand.

Slawski, M. and M. Hein (2015). Estimation of positive definite M-matrices and structure learning for attractive Gaussian Markov random fields. *Linear Algebra Appl. 473*, 145–179.

Smith, R. L., J. A. Tawn, and S. G. Coles (1997). Markov chain models for threshold exceedances. *Biometrika 84*(2), 249–268.

Spirtes, P., C. N. Glymour, R. Scheines, and D. Heckerman (2000). *Causation, prediction, and search*. MIT press.

Steel, M. (2016). *Phylogeny: discrete and random processes in evolution*. SIAM.

Stellato, B., G. Banjac, P. Goulart, A. Bemporad, and S. Boyd (2020). OSQP: an operator splitting solver for quadratic programs. *Mathematical Programming Computation 12*(4), 637–672.

Sturmfels, B., C. Uhler, and P. Zwiernik (2020). Brownian motion tree models are toric. *Kybernetika (Prague) 56*(6), 1154–1175.

Tawn, J. A. (1990). Modelling multivariate extreme value distributions. *Biometrika 77*, 245–253.

Tran, N. M., J. Buck, and C. Klüppelberg (2021). Estimating a latent tree for extremes. *arXiv preprint arXiv:2102.06197*.

Vinicius, Z. and D. Palomar (2019). *spectralGraphTopology: Learning Graphs from Data via Spectral Constraints*. Available from `https://cran.r-project.org/package=spectralGraphTopology`.

Vinicius, Z., J. Ying, and D. Palomar (2021). *sparseGraph: Estimating Graphs with Nonconvex, Sparse Promoting Regularizations*. Available from `https://github.com/mirca/sparseGraph/`.

Wadsworth, J. L. and J. A. Tawn (2012). Dependence modelling for spatial extremes. *Biometrika 99*(2), 253–272.

Wainwright, M. J. and M. I. Jordan (2008). Graphical models, exponential families, and variational inference. *Foundations and Trends in Machine Learning 1*, 1–305.

Wang, Y., U. Roy, and C. Uhler (2020). Learning high-dimensional Gaussian graphical models under total positivity without adjustment of tuning parameters. In S. Chiappa and R. Calandra (Eds.), *Proceedings of the Twenty Third International Conference on Artificial Intelligence and Statistics*, Volume 108 of *Proceedings of Machine Learning Research*, pp. 2698–2708. PMLR.

Ying, J., J. M. Cardoso, and D. Palomar (2021). Minimax estimation of Laplacian constrained precision matrices. In *International Conference on Artificial Intelligence and Statistics*, pp. 3736–3744. PMLR.

Zhao, L., Y. Wang, S. Kumar, and D. Palomar (2019). Optimization algorithms for graph Laplacian estimation via ADMM and MM. *IEEE Transactions on Signal Processing 67*(16), 4231–4244.

Zwiernik, P. (2018). Latent tree models. In *Handbook of Graphical Models*, pp. 265–288. CRC Press.